

1 **Exploration of the circulating human secretome through protein quantitative trait analysis**
2 **identifies an association between circulating levels of apolipoprotein L1 and risk of giant**
3 **cell arteritis**

4 **Authors:**

5 NJM Chaddock¹, M Zulcinski^{1,2}, J Martin³, A Mälarstig⁴, JE Peters⁵, MM Iles^{1,2}, AW Morgan^{1,2,6}
6 on behalf of the UK GCA Consortium

7 **Affiliations:**

8 ¹ School of Medicine, University of Leeds, UK

9 ² NIHR Leeds Biomedical Research Centre, Leeds Teaching Hospitals NHS Trust, Leeds, UK

10 ³ Institute of Parasitology and Biomedicine López-Neyra, CSIC, Spain

11 ⁴ Department of Medical Epidemiology and Biostatistics, Karolinska Institutet, Stockholm,
12 Sweden

13 ⁵ Department of Immunology and Inflammation, Faculty of Medicine, Imperial College London,
14 London, UK

15 ⁶ NIHR Leeds Medicines and In Vitro Diagnostics Co-operative, Leeds Teaching Hospitals NHS
16 Trust, Leeds, UK

17 ⁷ See Appendix 1 for members of the UK GCA Consortium

18

19 **Apolipoprotein-L1 association with giant cell arteritis**

20

21 **Corresponding author:**

22 Ann W Morgan, a.w.morgan@leeds.ac.uk, Leeds Institute of Cardiovascular and Metabolic
23 Medicine, School of Medicine, LIGHT Building, Clarendon Way, University of Leeds, Leeds
24 LS2 9DA, UK

25

26 **Total word count: 8244**

27

28 **Abstract**

29 **Background**

30 Glucocorticoid monotherapy remains the principal treatment for giant cell arteritis (GCA), yet
31 concurrent toxicity and adverse effects highlight the need for targeted therapies and improved
32 risk stratification. Previous work suggests that evidence of genetic association can improve
33 success rates in clinical trials and identify biomarkers for risk assessment, particularly when
34 combined with other ‘omics data, such as proteomics. However, relatively little is currently
35 known about the genetic basis of GCA.

36 **Methods**

37 Polygenic risk scores (PRS) were developed for 169 human plasma proteins and tested for
38 association with GCA susceptibility (cases $N=729$, controls $N=2,619$). Associated PRS were
39 replicated in an independent cohort (cases $N=1,129$, controls $N=2,654$) and their respective
40 proteins were evaluated for causality using Mendelian randomization (MR). Finally,
41 relationships between proteins with GCA-associated PRS were assessed using protein-protein
42 interaction (PPI) network analysis

43 **Results**

44 The Apolipoprotein L1 (APOL1) PRS had a statistically significant GCA association with a
45 protective effect ($P\text{-value}[P]=1 \times 10^{-4}$), which replicated in an independent dataset ($P=8.69 \times 10^{-4}$),
46 and MR analysis supported a causal relationship ($\beta=-0.093$; $SE=0.02$; $P=4.42 \times 10^{-9}$). PPI
47 network analysis of proteins with GCA-associated PRS revealed enrichment for “negative
48 regulation of fibrinolysis” and “negative regulation of blood coagulation” pathways.

49 **Conclusions**

50 This work emphasizes a potentially protective role of APOL1 and therefore reverse cholesterol
51 transport in the pathogenesis of GCA. These findings also implicate fibrinolytic and coagulation
52 cascades in GCA susceptibility, highlighting pathways that may be of interest for future
53 pharmaceutical targeting.

54

55 **Non-standard Abbreviations and Acronyms**

56 GCA, giant cell arteritis; MHC, major histocompatibility complex; GWAS, genome-wide
57 association study; SNPs, single nucleotide polymorphisms; PRS, polygenic risk score; pQTL,
58 protein quantitative trait loci; MR, Mendelian randomization; QC, quality control; WTCCC,
59 Wellcome Trust Case Control Consortium; PCA, principal component analysis; IV, instrumental
60 variables; IVW, inverse-variance weighted; PheWAS, phenome-wide association study; GO,
61 gene ontology; FUMA, Functional Mapping and Annotation of Genome-Wide Association
62 Studies; MAGMA, Multi-marker Analysis of GenoMic Annotation; RCT, reverse cholesterol
63 transport.

64

65 **Clinical Perspective**

66 **What is new?**

- 67
- 68 • An apolipoprotein-L1 polygenic risk score was associated with giant cell arteritis
susceptibility, and replicated in an independent dataset.

- 69 • Evidence for causality of a protective effect of apolipoprotein-L1 in giant cell arteritis
70 susceptibility was identified using Mendelian randomization.
- 71 • Proteins with giant cell arteritis-associated polygenic risk scores were enriched in
72 coagulation-related, fibrinolytic and immune response pathways.

73 **What are the clinical implications?**

- 74 • Findings from this study indicate a protective role of apolipoprotein-L1 in giant cell
75 arteritis susceptibility, highlighting a potential involvement of reverse cholesterol
76 transport and lipid metabolism in disease pathogenesis.
- 77 • Fibrinolytic and coagulation cascades were also implicated in the disease in addition to
78 innate immune response pathways, redrawing attention to the role of
79 thromboinflammation and the need to re-evaluate anti-platelet and anticoagulant
80 therapies, particularly for those with impending visual loss and cranial ischaemic
81 complications.

82 **Introduction**

83 Giant cell arteritis (GCA) is a medium- and large-vessel vasculitis which overwhelmingly arises
84 in individuals aged ≥ 50 years¹. GCA is characterized by chronic vascular inflammation (often of
85 cranial arteries) and intimal hyperplasia, resulting in arterial stenoses and downstream ischaemic
86 tissue damage, resulting in clinical manifestations such as sight loss, stroke and scalp necrosis, as
87 well as late aortic dilatation and aneurysm formation².

88 High incidence rates in populations of Scandinavian descent, not entirely explained by
89 environmental factors, and clustering of familial cases, are indicative of a genetic component to
90 GCA^{1,3}. This is supported by candidate gene studies, which identified genetic associations with
91 GCA in genes of the *major-histocompatibility complex (MHC)*⁴, cytokine genes⁵, and genes with
92 known vascular functions⁶. The largest systematic investigation into the genetic basis of GCA to
93 date is a genome-wide association study (GWAS) on a cohort of 2,134 case and 9,125 control
94 subjects. This study confirmed independent associations in *HLADRB1* and *HLADQA1* in the
95 HLA class II region, alongwith *HLA B* and identified two novel loci related to GCA
96 susceptibility: the *PLG* and *P4HA2* genes, which play important roles in vascular remodelling
97 and angiogenesis, processes previously hypothesised to be involved in the pathogenesis of
98 GCA⁷.

99 However, given that GCA has a complex, polygenic aetiology, individual genome-wide
100 significant ($P\text{-value}[P] \leq 5 \times 10^{-8}$) variants explain just a small proportion of disease propensity.
101 Previous work investigating complex diseases suggests that genetic risk may be better captured
102 by combining small-effect single nucleotide polymorphisms (SNPs) into a single polygenic risk
103 score (PRS)⁸, which estimates an individual's propensity to a phenotype by summarising multiple
104 risk alleles carried by an individual, weighted by effect sizes from GWAS summary statistics.

105 Glucocorticoid monotherapy (usually prednisone) is the principle treatment option for GCA.
106 Research has indicated that whilst glucocorticoid therapy is successful in reducing symptoms of
107 GCA, many patients relapse when tapering glucocorticoid doses or following cessation of
108 treatment. Because of this, patients often remain on low-dose glucocorticoid therapy for many
109 years and experience adverse effects such as osteoporosis, infections, hypertension and
110 gastrointestinal bleeding⁹. Tocilizumab (targeting the interleukin-6 receptor, IL-6R) is a licenced
111 therapy, but access is restricted in many healthcare systems⁹, and not all patients can tolerate this
112 therapy¹⁰. Thus, there is ongoing unmet need for novel targeted therapies and improved
113 biomarkers for risk stratification to induce and maintain remission of GCA.

114 It has been demonstrated that a drug with additional genetic support is twice as likely to proceed
115 from phase I clinical trials to approval^{11, 12}. Therefore, using genetic data to guide drug discovery
116 could reduce rates of failure in clinical development caused by poor drug efficacy, particularly
117 when genetic data are enriched with other types of ‘omics information, such as proteomics¹³. By
118 doing so, it may be possible to identify proteins implicated in the pathogenesis of GCA and
119 provide a basis for pharmaceutical targeting and biomarker identification.

120 For example, recent developments in high-throughput technologies and the emergence of
121 genome-wide methodology have allowed groups to perform large-scale protein quantitative trait
122 loci (pQTL) analyses and subsequent causality estimation with Mendelian randomisation (MR)¹³,
123 ¹⁴. Such work has identified inherited variation in protein levels which could provide the link
124 between germline genetic variants and disease phenotypes, given that proteins are often the
125 molecules directly implicated in pathogenic cascades.

126 In this study, we constructed PRS for several blood secretome proteins and tested these for
127 association with GCA. We used MR to test for causality of these proteins and suggest novel
128 biomarkers for drug repurposing or patient stratification.

129 **Methods**

130 Protein selection

131 Circulating plasma proteins with publicly available summary statistics, generated from GWAS
132 investigating inter-individual variation in protein levels, were selected for study in this work¹³.
133 To prioritise the proteins investigated and minimise multiple testing, two filters were applied to
134 the selection of plasma proteins for inclusion in the study. Firstly, 730 proteins deemed part of
135 the “human blood secretome” were selected, based on prior knowledge that circulating proteins
136 represent useful druggable targets and because their primary physiological action is in circulating
137 form¹⁵. Secondly, proteins with low estimated levels of heritability ($R^2 \leq$ lowest quartile),
138 therefore underpowered to demonstrate strong genetic associations with GCA-risk, were
139 removed from the study. Following these filters, 169 proteins remained for subsequent analysis
140 **(Supplementary Methods)**.

141 Quality control of giant cell arteritis datasets

142 Cases from UK GCA consortium ($N=1,858$) and controls from Wellcome Trust Case-Control
143 Consortium (WTCCC; $N=3,748$), were used to develop PRS for blood secretome proteins in this
144 work. Information regarding the quality control (QC) of both GCA and Wellcome Trust Case
145 Control Consortium (WTCCC) genotype data may be found in **Supplementary Methods**.
146 Briefly, genotyping was performed using the Illumina “Infinium HumanCore Beadchip” and
147 “Infinium Global Screening” arrays (UK GCA cases) and Illumina 1.2M custom chip (WTCCC

148 controls, late summer 2009 release). Sample and variant QC were executed in PLINK v1.07¹⁶,
149 including the use of principal component analysis (PCA) to account for population stratification
150 **(Supplementary Methods)**.

151 This cohort was divided into two subsets. The first comprised 729 GCA cases and 2,619
152 WTCCC controls (from the 1958 British Birth Cohort), and was used to optimize protein PRS
153 and test for their association with GCA susceptibility.

154 The second subset was used for PRS replication in this work, formed from a cohort of 1,129 UK
155 GCA consortium cases and 2,654 WTCCC controls (from the UK Blood Service control group).

156 Polygenic risk scoring

157 The PRSice v2.3.3¹⁷ software was used for developing protein PRS and testing for associations
158 with GCA. PRS were constructed via the “clumping and thresholding” approach, using effect
159 sizes and *P-values* from GWAS of protein levels¹³, and tested for association with GCA
160 susceptibility in the primary sub-cohort using logistic regression ($GCA \sim PRS + PCI-10$;
161 **Supplementary Methods**). To account for population stratification, the top 10 principal
162 components (PCs) from PCA were included as covariates. The “optimal” PRS was defined as
163 that PRS with the greatest Nagelkerke¹⁸ R^2 value in logistic regression.

164 To account for multiple testing, the significance threshold was adjusted for the number of
165 proteins tested using Bonferroni correction. For the 169 proteins assessed by PRS analysis, the
166 corrected *P-value* threshold was $0.05/169=2.96 \times 10^{-4}$.

167 Details of additional sensitivity analyses, including testing of associated PRS for different case
168 definitions, and different GCA severity outcomes, may be found in **Supplementary Methods**
169 **(Supplementary Table 1)**.

170 Replication was performed using the secondary sub-cohort. SNPs and weights from GCA-
171 associated protein PRS were used to calculate PRS in an independent dataset with PRSice
172 v2.3.3¹⁷, and these PRS were tested for association with GCA in logistic regression, using the top
173 10 PCs from PCA as covariates ($GCA \sim PRS + PCI-10$). PRS were calculated using SNPs from
174 data unfiltered for imputation quality. This was in order to capture as many SNPs as possible
175 from PRS developed in the primary analyses, thereby reproducing PRS as accurately as possible.
176 99.98% of imputed SNPs in these PRS had an imputation quality $R^2 > 0.3$, and no SNP had an
177 $R^2 < 0.04$.

178 Testing polygenic risk scores for association with off-target proteins

179 Use of SomaLogic aptamers in protein quantification holds potential for cross-reactivity with
180 off-target proteins. Therefore, where possible, PRS with statistically significant associations with
181 GCA were tested for association with proteins found in complex with target proteins (identified
182 using a literature search), to assess whether PRS were predictive of these protein levels instead of
183 intended targets. Protein quantification data was obtained from UK Biobank¹⁹ and tested for
184 association with the relevant PRS using linear regression in up to 350,883 white European UK
185 Biobank participants, adjusting for the top 10 PCs from PCA as covariates. Details of UK
186 Biobank QC and PCA may be found in **Supplementary Methods**.

187 Mendelian randomization

188 Proteins with GCA susceptibility-associated PRS were further evaluated using MR, to assess
189 whether their associations with GCA represent a causal relationship. MR is a statistical technique
190 which uses genetic variants as instrumental variables (IV) to assess whether ‘exposures’ (here,
191 proteins) are causally associated with an outcome (here, GCA).

192 Using summary statistics from respective GWAS of plasma protein levels¹³, three genetic scores
193 were constructed as IVs (following the pruning of SNPs with linkage disequilibrium $R^2 > 0.1$).
194 IVs were then used to tested for an association between the protein and GCA susceptibility in
195 MR, using summary statistics from a GCA GWAS. The three scores for each tested protein
196 used a different *P-value* threshold to filter SNPs for inclusion in the IV. These included: a
197 “liberal” score (*P-value* threshold as defined by the optimal PRS in the clumping and
198 thresholding approach), an “intermediate” score (*P-value* threshold $\leq 5 \times 10^{-5}$), and a
199 “conservative” score (*P-value* threshold $\leq 5 \times 10^{-8}$).

200 Two-sample MR was performed using the inverse-variance weighted (IVW) method, and the
201 measure of variance used was standard error (SE). Sensitivity analyses (including Cochran’s
202 heterogeneity test, MR-Egger intercept test, and weighted median and mode MR methods) were
203 performed to rule out potential horizontal pleiotropy, which could invalidate use of the genetic
204 instruments¹⁴. If IVs yielded evidence for potential pleiotropy in sensitivity analyses, SNPs from
205 that IV were further investigated using a phenome-wide association study (PheWAS) approach
206 **(Supplementary Methods)**.

207 Protein-protein interaction network analysis

208 Proteins with associated PRS were tested for protein-protein interaction enrichment using
209 StringDB v12.0²⁰. StringDB utilizes multiple sources of evidence (e.g. experimental,
210 coexpression, and text mining) as priors to assess the probability of two proteins being functional
211 interactors. Enrichment of gene ontology (GO) processes for proteins in this network were also
212 tested²¹.

213 Pathway analyses

214 The Functional Mapping and Annotation of Genome-Wide Association Studies (FUMA) v1.4.0
215 tool²² was used to perform pathway analysis on protein PRS associated with GCA. FUMA is a
216 package which combines several *in-silico* tools (including the Multi-marker Analysis of
217 GenoMic Annotation (MAGMA) gene-based test²³) to provide functional interpretation of SNPs
218 in PRS.

219

220 **Results**

221 Polygenic risk scoring

222 We developed PRS for 169 proteins/protein complexes of the human blood secretome. Of these
223 PRS, 12 reached $P < 0.05$ prior to multiple testing adjustment (**Figure 1**), whilst one protein,
224 apolipoprotein-L1 (APOL1), remained significant at $P = 2.96 \times 10^{-4}$ following Bonferroni
225 correction (**Table 1**).

226 The APOL1 PRS had a statistically significant association with GCA susceptibility ($P = 1 \times 10^{-4}$),
227 following Bonferroni correction. This PRS consisted of 2,278 SNPs distributed across the
228 genome, two of which (rs117674301 and rs117850190) were classed as *cis*-pQTL, whilst most
229 had *trans* effects on APOL1 levels. The PRS had a negative coefficient ($coefficient[SE] = -$
230 $53.36[10.03]$), indicating that a PRS which increases levels of APOL1 is associated with reduced
231 risk of GCA (**Figure 2**). The variance in GCA susceptibility explained by the risk score is
232 estimated at approximately 0.8% (Nagelkerke's $R^2 = 0.008$). Results of high-resolution PRS for
233 APOL1, testing the APOL1 PRS in different case definitions, and testing for association between
234 APOL1 and secondary outcomes may be found in **Supplementary Results (Supplementary**
235 **Figures 1-2; Supplementary Table 2)**.

236 PRS associated with GCA susceptibility passing the P -value <0.05 are summarised in
237 **Supplementary Results (Table 1)**. Briefly, these associations included PRS for the
238 superoxidase dismutase protein (*coefficient* [SE]=15.36 [4.02]; $P=4\times 10^{-3}$), C1 inhibitor protein
239 (*coefficient*[SE]=382.35[112.25]; $P=0.01$), and plasminogen protein (*coefficient*[SE]=0.83[0.25];
240 P -value=0.01).

241 Replication of the APOL1 PRS association was performed in an independent GCA dataset
242 comprising 1,129 cases and 2,654 controls. Of the 2,278 SNPs in the initial PRS, 2,261 were
243 present in the second dataset (**Table 1**). Following adjustment for 10 PCs, the APOL1 PRS had a
244 statistically significant association with GCA with a negative direction of effect
245 (*coefficient*[SE]=-27.43[8.23], $P=8.69\times 10^{-4}$), consistent with that found for the association in the
246 primary cohort.

247 Furthermore, 11 other protein PRS with P -value <0.05 were tested for replication, revealing two
248 associations: the plasminogen PRS ($R^2=0.019$; *coefficient*[SE]=-2.25[0.20]; $P=1.62\times 10^{-28}$) and
249 the vitronectin PRS ($R^2=0.001$; *coefficient*[SE]=-46.42[17.23]; $P=7.07\times 10^{-3}$).

250 Testing polygenic risk scores for association with off-target proteins

251 To determine whether the APOL1 PRS is associated with off-target proteins, it was tested for
252 association with APOA1 blood plasma levels (UK Biobank nuclear magnetic resonance
253 measurements) in a linear regression utilising 350,883 UK Biobank subjects. No association was
254 found between the APOL1 PRS and APOA1 (*coefficient*=-0.34; $SE=0.65$; $P=0.60$), suggesting
255 that the PRS is not predictive of APOA1 levels.

256 Mendelian randomization

257 Once effect and non-effect alleles were harmonised between the exposure (APOL1) and outcome
258 (GCA susceptibility) data, MR analysis was performed using each of the three risk scores
259 constructed for use as APOL1 IVs. Using the IVW method of MR, the APOL1 protein was
260 estimated by all risk scores to have a statistically significant, causal effect on GCA susceptibility
261 (**Supplementary Table 3; Supplementary Figure 3**). The direction of effect was negative in
262 each instance (liberal $\beta[SE]=-0.093[0.02]$; intermediate $\beta[SE]=-0.131[0.05]$; conservative
263 $\beta[SE]=-0.22[0.1]$), and was supported by the weighted median and weighted mode methods of
264 MR. Details of MR sensitivity analyses may be found in **Supplementary Results**
265 (**Supplementary Tables 4-7**). Briefly, results of the MR-Egger intercept test lacked statistical
266 significance for any of the risk scores, and following the repetition of MR with three potentially
267 pleiotropic SNPs removed from the score, the causal effect of the APOL1 protein on GCA
268 susceptibility remained statistically significant for each of the risk scores. This indicates a lack of
269 evidence to suggest that pleiotropic SNPs are confounding the association observed here.

270 Protein-protein interaction network analysis

271 To understand relationships between proteins with GCA susceptibility-associated PRS, we
272 performed protein-protein interaction [PPI] network analysis (**Figure 3**). Significantly more
273 interactions were observed across the 12-protein network than expected by chance (nodes $N=12$,
274 edges $N=6$, expected edges $N=1$, PPI enrichment $P=1.61 \times 10^{-4}$). The most significantly enriched
275 GO processes for proteins in this network included “negative regulation fibrinolysis” (pathway
276 protein [PP] $N=13$, network protein [NP] $N=2$, *false discovery rate*[FDR]=0.04), and “negative
277 regulation of blood coagulation” (PP $N=46$, NP $N=4$, $FDR=2.8 \times 10^{-4}$).

278 Pathway analyses

279 Pathway analyses were performed on the 2,278 SNP APOL1 PRS. Using the MAGMA gene-
280 based test²³, input SNPs were assigned to protein-coding genes ($N=19,054$), revealing 14 genes
281 significantly enriched for SNPs in the APOL1 PRS at the Bonferroni corrected P -value
282 $0.05/19,054=2.62 \times 10^{-6}$ (**Table 2; Figure 4**), including: *DNMBP* (z -stat=8.34; $P=3.81 \times 10^{-17}$),
283 *LRRC15* (z -stat=7.75; $P=4.77 \times 10^{-15}$), *CPN1* (z -stat=6.11; $P=5 \times 10^{-10}$), and *CPN2* (z -stat=6.11;
284 $P=5 \times 10^{-10}$).

285 When proteins encoded by these genes were added to the protein-protein interaction network
286 analysis, significantly more interactions were observed across the 25 proteins than would be
287 expected by chance (nodes $N=25$, edges $N=14$, expected edges $N=2$, PPI enrichment P -
288 value= 1.69×10^{-9}). The most significantly enriched GO processes for proteins in this network
289 included “negative regulation of blood coagulation” (PP $N=46$, NP $N=4$, $FDR=7 \times 10^{-3}$), and
290 “immune response” (PP $N=1,321$, NP $N=9$, $FDR=0.04$).

291 **Discussion**

292 Here, we performed a systematic evaluation testing genetically-determined levels of circulating
293 proteins against GCA susceptibility. We found evidence for an association between a 2,278 SNP
294 APOL1 PRS and GCA, which replicated in an independent cohort. Further evaluation with MR
295 revealed evidence for causal effect on disease risk, with genetic tendency to higher levels of
296 APOL1 plasma protein associated with reduced risk of GCA. These results are suggestive of a
297 potentially protective role for circulating APOL1 protein in GCA and highlight a shared genetic
298 aetiology of the protein and GCA.

299 This association emphasises the potential benefits of integrating genomic and proteomic data
300 when searching for novel pathogenic mechanisms, and hence potential therapeutic targets, in

301 disease. Pairing genetic information with protein data allows not only the identification of an
302 association between proteins and disease, but enables the discovery of common biological
303 pathways influencing both protein levels and disease pathogenesis, providing more research
304 avenues for the identification of novel therapeutic targets and risk stratification biomarkers.

305 APOL1 arose from a gene duplication event approximately 30 million years ago and is present in
306 some higher primate species and humans, but not other mammals²⁴. It is an innate immune
307 effector which integrates into protein complexes and circulates in blood plasma bound to high
308 density lipoprotein (HDL) particles or complexed to IgM²⁵. It is thought to have roles in
309 protection against pathogens, inflammation, lipid binding/transport (including cardiolipins),
310 cholesterol metabolism, and cardiovascular disease^{25, 26}.

311 Much of our biological knowledge of APOL1 is derived from studies of recessive gain of
312 function *APOLI* variants that emerged in Sub-Saharan Africa, which conferred protection from
313 pathogenic trypanosomes. Approximately 13% of African Americans have two copies of risk
314 alleles, which explains most of the excess risk of non-diabetic kidney disease in individuals of
315 African descent, particularly hypertensive end-stage kidney disease and focal segmental
316 glomerulosclerosis, but also lupus-related nephropathy. Poor renal transplant outcomes observed
317 when the donor tissue, rather than recipient, has the *APOLI* risk haplotypes, suggests the poor
318 renal outcomes are likely to be due to a tissue phenotype rather than circulating APOL1 levels²⁴.

319 Although the APOL1 protein is found in kidney tissue, the majority of APOL1 in humans is
320 found circulating in serum or located in vascular tissue²⁷. Previous work has suggested that
321 plasma APOL1 levels are not associated with kidney function, but do correlate with fasting
322 lipids, suggesting that the source of APOL1 is unlikely to be from kidney tissue^{28, 29}. Proteomics
323 approaches have demonstrated that APOL1 circulates as part of two specialized complexes

324 which form a minor HDL subfraction. In the first, APOL1 is bound to cholesterol, cholesterol
325 esters, phospholipids, haptoglobin-related protein (HPR), haemoglobin and another
326 apolipoprotein, APOA1, forming a complex termed trypanosome lytic factor-1 (TLF1). In the
327 second, APOL1 is found as part of a complex again containing APOA1 and HPR, but also
328 immunoglobulin M and fibronectin, termed TLF2²⁵.

329 Interestingly, TLF complexes and APOL1 have proposed functions in HDL metabolism, and are
330 linked to susceptibility to CVDs²⁵. As previously established, APOL1 is a minor protein
331 component of HDL and is expressed in human vascular cells. Important roles of HDL are
332 thought to be reverse cholesterol transport (RCT) from peripheral tissues to the liver, and
333 promotion of nitric oxide production by endothelial cells, resulting in anti-apoptotic/anti-
334 inflammatory effects and a reduction in atherosclerotic risk³⁰. Previous work has found that
335 African ancestry risk variants APOL1-G1 and -G2 (which are thought to negatively impact
336 APOL1 function and are found in low frequencies in European populations with minor allele
337 frequency 0.000242 and 0.00013, respectively^{31,32}), result in impaired RCT via reduction in
338 expression of cholesterol efflux transporters³³; thus providing evidence for the role of APOL1 in
339 RCT. It has been proposed that with impaired RCT, lipid accumulation, macrophage
340 transformation into foam cells and release of inflammatory factors occur, creating a pro-
341 inflammatory state which could lead to increased ischaemic risk.

342 The impact of APOL1 levels on impaired RCT is supported by evidence that found low serum
343 levels of APOL1, along with low HDL-bound APOL1 levels (affecting HDL composition, but
344 not total HDL levels) in subjects with familial hyperlipidemia, suggesting that low volumes of
345 APOL1 may reduce RCT and result in increased cholesterol/lipid levels in individuals.

346 Additionally, the study found that low APOL1 levels were predictive of ischaemic cardiac

347 events, and that APOL1/HDL-cholesterol ratios were predictive of post-event survival rates³⁴. It
348 is therefore possible that impaired cholesterol transport and subsequent lipid accumulation,
349 atherosclerosis and inflammatory mediator release could represent a mechanism through which
350 low heritable APOL1 levels may contribute to the increased vascular inflammation found in
351 GCA patients.

352 Because APOL1 is almost exclusively found bound to complexes with the APOA1 protein, it
353 was important to ensure that the PRS found to be associated with GCA in this work was
354 predictive of levels of APOL1 in blood plasma, and not APOA1. To test this, the APOL1 PRS
355 developed in this work was tested for association with APOA1 levels in UK Biobank data. No
356 association was found between the PRS and APOA1 levels, indicating that the PRS is likely
357 predictive of APOL1 levels, and not APOA1, in the plasma.

358 In addition to the APOL1 PRS, a small number of PRS had associations at the $p \leq 0.05$ level, but
359 did not yield statistical strength to pass the multiple testing threshold. Of these results, two PRS
360 replicated in an independent cohort: vitronectin PRS and plasminogen PRS, providing evidence
361 that these proteins may also be implicated in GCA susceptibility, supporting previous findings
362 from GWAS³⁵. Protein-protein interaction network analysis of these proteins using StringDB²⁰
363 revealed biological pathways enriched for proteins in the network, including “negative regulation
364 of fibrinolysis”, “negative regulation of blood coagulation” and “immune response” pathways.

365 When proteins encoded by genes enriched for SNPs in the APOL1 PRS were added to the
366 protein-protein interaction network, both the “negative regulation of blood coagulation” and
367 “immune response” pathways remained enriched, and a 10-protein network was formed,
368 including vitronectin, plasminogen, C1 inhibitor, coagulation factor X and multiple
369 apolipoproteins. Notably, this network links apolipoprotein L1 to the vitronectin-plasminogen

370 network through apolipoprotein C2, a protein which plays a known role in lipoprotein
371 metabolism and has recently been implicated in Takayasu arteritis³⁶. These findings may suggest
372 a link between both lipid metabolism and coagulation cascades, and the development of GCA,
373 and highlight a number of new potential biomarkers for future study. Indeed, given prior
374 speculation over the role of anti-coagulants in reducing risk of cranial ischaemic complications
375 in GCA³⁷, it is prudent that these pathways are further interrogated using functional and multi-
376 omics studies to untangle the relationship between fibrinolytic/coagulation cascades and GCA
377 progression.

378 Limitations

379 Findings from this study must be interpreted in light of some limitations. This work's primary
380 drawback concerns its limited sample size. A small cohort can restrict power, meaning that
381 variants of small effect may be missed (although this was combated using a PRS approach).
382 Furthermore, two filters were applied during selection of plasma proteins, in order to reduce the
383 number of tested hypotheses. However, by limiting the number of proteins studied, molecules
384 important in the pathogenesis of GCA may have been overlooked. For example, only proteins
385 present in the blood secretome were retained for analysis, and some molecules implicated in
386 GCA (such as JAK2)³⁸ were excluded for this reason. It may therefore be beneficial to repeat
387 analyses using a wider range of proteins in future studies utilising larger cohorts.

388 A further limitation of the work concerns the replication of the APOL1 PRS in an independent
389 cohort. Whilst the PRS was developed using genetic data filtered for imputation quality, the
390 second cohort in which it was calculated did not have an imputation quality threshold applied.
391 This was in order to accurately replicate the developed PRS. However, the absence of this
392 threshold could have resulted in the inclusion of poorly imputed SNPs in the PRS, adding noise

393 to the PRS and potentially impacting power of the PRS-GCA association. Future work should
394 aim to disentangle the impact of these SNPs on APOL1 PRS performance and replicate these
395 findings in a third, independent cohort.

396 Finally, whilst MR is a useful statistical concept for generating causal estimates, it is dependent
397 on a number of assumptions. Previous work has indicated that whilst large risk scores can
398 improve MR results by increasing power, the validity of these risk scores may be reduced if the
399 SNPs are not true predictors of the exposure variable¹⁴. Traditionally, genome-wide significant
400 SNPs at the gene locus of the exposure are used to ascertain this; however, the purpose of this
401 study was to identify genome-wide pQTL that affect protein levels, so sole use of *cis*-pQTL
402 would be inappropriate. Instead, the combined power of *cis*- and *trans*-pQTL in a PRS should
403 provide sufficient statistical and biological justification for their use as IVs. Furthermore, two
404 additional risk scores, consisting solely of variants with greater evidence for association with
405 APOL1, were used to confirm results found by the initial analyses. Because little is known about
406 the aetiology of GCA, the second and third assumptions, which regard alternate pathways from
407 SNPs to GCA, were difficult to assess objectively. For this reason, MR was used primarily to
408 support PRS findings, and results from these analyses should not be interpreted alone.

409 Conclusion

410 In this study interrogating human secretome proteins using a PRS approach, a 2,278 SNP
411 APOL1 PRS was associated with GCA susceptibility, with further evidence for causality using
412 MR. The findings from this work has revealed possible insights into the pathogenesis of GCA,
413 and the APOL1 protein may represent a future biomarker therapeutic targeting. For the first time,
414 these findings highlight the potential roles of RCT and the trypanosome lytic factors in GCA

415 pathogenesis, and demonstrate the value of repurposing publicly available genetic data in
416 discovery work.

417

418

419 **Acknowledgements**

420 We thank all patients who participated in this study. All UK GCA Consortium group
421 members contributed to patient and data collection and were integral to the delivery of this
422 project. A list of group members can be found in Appendix 1, available online.

423

424 **Sources of funding**

425 This work was supported in part by the MRC “Treatment According to Response in Giant cell
426 arteritis” (TARGET) Partnership award, MRC DiMeN award, NIHR Leeds Biomedical
427 Research Centre.

428 The MRC TARGET Partnership award supported the salaries of AWM. AWM and MI were
429 supported by the NIHR Leeds Biomedical Research Centre, AWM was supported by the NIHR
430 Leeds MedTech and *In Vitro* Diagnostic Co-operative, NC was supported by an MRC DiMeN
431 PhD studentship and MZ was supported by the HELICAL European Union Horizon 2020
432 International Training Network. AWM is additionally supported through an NIHR Senior
433 Investigator award.

434 The views expressed are those of the author(s) and not necessarily those of the NHS, the NIHR
435 or the Department of Health and Social Care.

436

437 **Disclosures**

438 Contributorship: NJMC was responsible for the analysis planning, data collection, verification,
439 data analysis and manuscript writing of analyses in this work. AWM and MMI contributed to the
440 study conception and design. All authors contributed to the data interpretation, drafting and
441 critical revision of the article and approved the final submitted version.

442 Competing interests: The authors have no conflicts of interest for the work presented in this
443 manuscript.

444 Ethics approval: A favourable ethical opinion for the UK GCA Consortium (UK GCA) study
445 was granted by the Yorkshire and the Humber Leeds West Research Ethics Committee
446 (05/Q1108/28).

447 Data sharing: Data access requests should be directed to the corresponding author. We are unable
448 to share UK Biobank data but have included the variable names so that the study can be
449 reproduced. Generated PRS are available on request.

450

451

452 **Supplemental Material**

453 Supplemental Methods

454 Tables S1-S7

455 Figures S1-S3

456 References 39-50

457 Appendix 1

458

459 **References**

- 460 1. Salvarani CC, CS; O'Fallon, WM; Hunder, GG; Gabriel, SE. Reappraisal of the epidemiology of
461 giant cell arteritis in Olmsted County, Minnesota, over a fifty-year period. *Arthritis Rheum.* 2004;51:264-
462 268.
- 463 2. Dejaco C, Brouwer E, Mason JC, Buttgereit F, Matteson EL and Dasgupta B. Giant cell arteritis
464 and polymyalgia rheumatica: current challenges and opportunities. *Nat Rev Rheumatol.* 2017;13:578-
465 592.
- 466 3. Liozon EO, B; Rhaïem, K, et al. Familial aggregation in giant cell arteritis and polymyalgia
467 rheumatica: a comprehensive literature review including 4 new families. *Clin Exp Rheumatol.*
468 2009;27:S89-S94.
- 469 4. Gonzalez-Gay MR, B; Vilchez, JR, et al. Contribution of MHC class I region to genetic
470 susceptibility for giant cell arteritis. *Rheumatology (Oxford).* 2007;46:431-434.
- 471 5. Boiardi LC, B; Farnetti, E, et al. Interleukin-10 promoter polymorphisms in giant cell arteritis.
472 *Arthritis Rheum.* 2006;54:4011-4017.
- 473 6. Amoli MG-P, C; Llorca, J; Ollier, WE; Gonzalez-Gay, MA. Endothelial nitric oxide synthase
474 haplotype associations in biopsy-proven giant cell arteritis. *J Rheumatol.* 2003;30:2019-22.
- 475 7. Carmona FD, Vaglio A, Mackie SL, Hernández-Rodríguez J, Monach PA, Castañeda S, Solans R,
476 Morado IC, Narváez J, Ramentol-Sintas M, Pease CT, Dasgupta B, Watts R, Khalidi N, Langford CA,
477 Ytterberg S, Boiardi L, Beretta L, Govoni M, Emmi G, Bonatti F, Cimmino MA, Witte T, Neumann T, Holle
478 J, Schönau V, Sailler L, Papo T, Haroche J, Mahr A, Mouthon L, Molberg Ø, Diamantopoulos AP, Voskuyl
479 A, Brouwer E, Daikeler T, Berger CT, Molloy ES, O'Neill L, Blockmans D, Lie BA, McLaren P, Vyse TJ,
480 Wijmenga C, Allanore Y, Koeleman BPC, Barrett JH, Cid MC, Salvarani C, Merkel PA, Morgan AW,
481 González-Gay MA, Martín J, Callejas JL, Caminal-Montero L, Corbera-Bellalta M, De Miguel E, López JBD,
482 García-Villanueva MJ, Gómez-Vaquero C, Guijarro-Rojas M, Hidalgo-Conde A, Marí-Alfonso B, Berriochoa
483 AM, Zapico AM, Martínez-Taboada VM, Miranda-Fillooy JA, Monfort J, Ortego-Centeno N, Pérez-Conesa

484 M, Prieto-González S, Raya E, Fernández RR, Sánchez-Martín J, Sopeña B, Tío L, Unzurrunzaga A, Gough
485 A, Isaacs JD, Green M, McHugh N, Hordon L, Kamath S, Nisar M, Patel Y, Yee C-S, Stevens R, Nandi P,
486 Nandagudi A, Jarrett S, Li C, Levy S, Mollan S, Salih A, Wordsworth O, Sanders E, Roads E, Gill A, Carr L,
487 Routledge C, Culfear K, Nugaliyadde A, James L, Spimpolo J, Kempa A, Mackenzie F, Fong R, Peters G,
488 Rowbotham B, Masqood Z, Hollywood J, Gondo P, Wood R, Martin S, Rashid LH, Robinson JI, Morgan M,
489 Sorensen L, Taylor J, Carette S, Chung S, Cuthbertson D, Forbess LJ, Gewurz-Singer O, Hoffman GS,
490 Koenig CL, Maksimowicz-Mckinnon KM, McAlear CA, Moreland LW, Pagnoux C, Seo P, Specks U, Spiera
491 RF, Sreih A, Warrington KJ and Weisman M. A Genome-wide Association Study Identifies Risk Alleles in
492 Plasminogen and P4HA2 Associated with Giant Cell Arteritis. *The American Journal of Human Genetics*.
493 2017;100:64-74.

494 8. International Schizophrenia Consortium; Purcell SW, NR; Stone, JL; Visscher, PM; O'Donovan,
495 MC; Sullivan, PF; Sklar, P. Common polygenic variation contributes to risk of schizophrenia and bipolar
496 disorder. *Nature*. 2009;460:748-52.

497 9. Mackie SL, Dejaco C, Appenzeller S, Camellino D, Duftner C, Gonzalez-Chiappe S, Mahr A,
498 Mukhtyar C, Reynolds G, de Souza AWS, Brouwer E, Bukhari M, Buttgerit F, Byrne D, Cid MC, Cimmino
499 M, Direskeneli H, Gilbert K, Kermani TA, Khan A, Lanyon P, Luqmani R, Mallen C, Mason JC, Matteson EL,
500 Merkel PA, Mollan S, Neill L, Sullivan EO, Sandovici M, Schmidt WA, Watts R, Whitlock M, Yacyshyn E,
501 Ytterberg S and Dasgupta B. British Society for Rheumatology guideline on diagnosis and treatment of
502 giant cell arteritis. *Rheumatology (Oxford)*. 2020;59:e1-e23.

503 10. Stone JT, K; Dimonaco, S, et al. Trial of Tocilizumab in Giant-Cell Arteritis. *N Engl J Med*.
504 2017;377:317-328.

505 11. Nelson MR, Tipney H, Painter JL, Shen J, Nicoletti P, Shen Y, Floratos A, Sham PC, Li MJ, Wang J,
506 Cardon LR, Whittaker JC and Sanseau P. The support of human genetic evidence for approved drug
507 indications. *Nat Genet*. 2015;47:856-60.

508 12. Cook DB, D; Alexander, R, et al. Lessons learned from the fate of AstraZeneca's drug pipeline: a
509 five-dimensional framework. *Nat Rev Drug Discov*. 2014;13:419–431.

510 13. Sun BB, Maranville JC, Peters JE, Stacey D, Staley JR, Blackshaw J, Burgess S, Jiang T, Paige E,
511 Surendran P, Oliver-Williams C, Kamat MA, Prins BP, Wilcox SK, Zimmerman ES, Chi A, Bansal N, Spain
512 SL, Wood AM, Morrell NW, Bradley JR, Janjic N, Roberts DJ, Ouwehand WH, Todd JA, Soranzo N, Suhre K,
513 Paul DS, Fox CS, Plenge RM, Danesh J, Runz H and Butterworth AS. Genomic atlas of the human plasma
514 proteome. *Nature*. 2018;558:73-79.

515 14. Burgess S, Butterworth A and Thompson SG. Mendelian randomization analysis with multiple
516 genetic variants using summarized data. *Genet Epidemiol*. 2013;37:658-65.

517 15. Uhlén MK, MJ; Hober, A, et al. The human secretome. *Sci Signal*. 2019;12:eaaz0274.

518 16. Chang CC, Chow CC, Tellier LC, Vattikuti S, Purcell SM and Lee JJ. Second-generation PLINK: rising
519 to the challenge of larger and richer datasets. *Gigascience*. 2015;4:7.

520 17. Choi SW and O'Reilly PF. PRSice-2: Polygenic Risk Score software for biobank-scale data.
521 *Gigascience*. 2019;8.

522 18. Nagelkerke N. A Note on a General Definition of the Coefficient of Determination. *Biometrika*.
523 1991;78:691-692.

524 19. Bycroft C, Freeman C, Petkova D, Band G, Elliott LT, Sharp K, Motyer A, Vukcevic D, Delaneau O,
525 O'Connell J, Cortes A, Welsh S, Young A, Effingham M, McVean G, Leslie S, Allen N, Donnelly P and
526 Marchini J. The UK Biobank resource with deep phenotyping and genomic data. *Nature*. 2018;562:203-
527 209.

528 20. Szklarczyk DK, R; Koutrouli, M, et al. The STRING database in 2023: protein-protein association
529 networks and functional enrichment analyses for any sequenced genome of interest. *Nucleic Acids Res*.
530 2023;51:D638-D646.

531 21. Ashburner MB, CA; Blake, JA, et al. Gene ontology: tool for the unification of biology. *The Gene*
532 *Ontology Consortium*. 2000;25:25-29.

533 22. Watanabe K, Taskesen E, van Bochoven A and Posthuma D. Functional mapping and annotation
534 of genetic associations with FUMA. *Nat Commun*. 2017;8:1826.

535 23. de Leeuw CA, Mooij JM, Heskes T and Posthuma D. MAGMA: generalized gene-set analysis of
536 GWAS data. *PLoS Comput Biol*. 2015;11:e1004219.

537 24. Friedman DJ and Pollak MR. APOL1 and Kidney Disease: From Genetics to Biology. *Annu Rev*
538 *Physiol*. 2020;82:323-342.

539 25. Weckerle A, Snipes JA, Cheng D, Gebre AK, Reisz JA, Murea M, Shelness GS, Hawkins GA, Furdui
540 CM, Freedman BI, Parks JS and Ma L. Characterization of circulating APOL1 protein complexes in African
541 Americans. *J Lipid Res*. 2016;57:120-30.

542 26. Gutierrez OM, Judd SE, Irvin MR, Zhi D, Limdi N, Palmer ND, Rich SS, Sale MM and Freedman BI.
543 APOL1 nephropathy risk variants are associated with altered high-density lipoprotein profiles in African
544 Americans. *Nephrol Dial Transplant*. 2016;31:602-8.

545 27. Monajemi H, Fontijn RD, Pannekoek H and Horrevoets AJ. The apolipoprotein L gene cluster has
546 emerged recently in evolution and is expressed in human vascular tissue. *Genomics*. 2002;79:539-46.

547 28. Bruggeman LA, O'Toole JF, Ross MD, Madhavan SM, Smurzynski M, Wu K, Bosch RJ, Gupta S,
548 Pollak MR, Sedor JR and Kalayjian RC. Plasma apolipoprotein L1 levels do not correlate with CKD. *J Am*
549 *Soc Nephrol*. 2014;25:634-44.

550 29. Daneshpajouhnejad P, Kopp JB, Winkler CA and Rosenberg AZ. The evolving story of
551 apolipoprotein L1 nephropathy: the end of the beginning. *Nat Rev Nephrol*. 2022;18:307-320.

552 30. Rysz J, Gluba-Brzozka A, Rysz-Gorzynska M and Franczyk B. The Role and Function of HDL in
553 Patients with Chronic Kidney Disease and the Risk of Cardiovascular Disease. *Int J Mol Sci*. 2020;21.

554 31. Medicine NLo. Reference SNP (rs) Report: rs73885319. 2022.

555 32. Medicine NLo. Reference SNP (rs) Report: rs71785313. 2022.

556 33. Ryu JH, Ge M, Merscher S, Rosenberg AZ, Desante M, Roshanravan H, Okamoto K, Shin MK,
557 Hoek M, Fornoni A and Kopp JB. APOL1 renal risk variants promote cholesterol accumulation in tissues
558 and cultured macrophages from APOL1 transgenic mice. *PLoS One*. 2019;14:e0211559.

559 34. Cubedo J, Padro T, Alonso R, Mata P and Badimon L. ApoL1 levels in high density lipoprotein and
560 cardiovascular event presentation in patients with familial hypercholesterolemia. *J Lipid Res*.
561 2016;57:1059-73.

562 35. Carmona FV, A; Mackie, SL, et al. A Genome-wide Association Study Identifies Risk Alleles in
563 Plasminogen and P4HA2 Associated with Giant Cell Arteritis. *Am J Hum Genet*. 2017;100:64-74.

564 36. Tamura N, Maejima Y, Shiheido-Watanabe Y, Nakagama S, Isobe M and Sasano T. Plasma
565 apolipoprotein C-2 elevation is associated with Takayasu arteritis. *Sci Rep*. 2021;11:18958.

566 37. Lee MS, SD; Galor, A; Hoffman, GS. Antiplatelet and anticoagulant therapy in patients with giant
567 cell arteritis. *Arthritis Rheum*. 2006;54:3306-3309.

568 38. Zhang H, Watanabe R, Berry GJ, Tian L, Goronzy JJ and Weyand CM. Inhibition of JAK-STAT
569 Signaling Suppresses Pathogenic Immune Responses in Medium and Large Vessel Vasculitis. *Circulation*.
570 2018;137:1934-1948.

571 39. Das S, Forer L, Schonherr S, Sidore C, Locke AE, Kwong A, Vrieze SI, Chew EY, Levy S, McGue M,
572 Schlessinger D, Stambolian D, Loh PR, Iacono WG, Swaroop A, Scott LJ, Cucca F, Kronenberg F, Boehnke
573 M, Abecasis GR and Fuchsberger C. Next-generation genotype imputation service and methods. *Nat*
574 *Genet*. 2016;48:1284-1287.

575 40. Taliun D, Harris DN, Kessler MD, Carlson J, Szpiech ZA, Torres R, Taliun SAG, Corvelo A, Gogarten
576 SM, Kang HM, Pitsillides AN, LeFaive J, Lee SB, Tian X, Browning BL, Das S, Emde AK, Clarke WE, Loesch
577 DP, Shetty AC, Blackwell TW, Smith AV, Wong Q, Liu X, Conomos MP, Bobo DM, Aguet F, Albert C,
578 Alonso A, Ardlie KG, Arking DE, Aslibekyan S, Auer PL, Barnard J, Barr RG, Barwick L, Becker LC, Beer RL,

579 Benjamin EJ, Bielak LF, Blangero J, Boehnke M, Bowden DW, Brody JA, Burchard EG, Cade BE, Casella JF,
580 Chalazan B, Chasman DI, Chen YI, Cho MH, Choi SH, Chung MK, Clish CB, Correa A, Curran JE, Custer B,
581 Darbar D, Daya M, de Andrade M, DeMeo DL, Dutcher SK, Ellinor PT, Emery LS, Eng C, Fatkin D, Fingerlin
582 T, Forer L, Fornage M, Franceschini N, Fuchsberger C, Fullerton SM, Germer S, Gladwin MT, Gottlieb DJ,
583 Guo X, Hall ME, He J, Heard-Costa NL, Heckbert SR, Irvin MR, Johnsen JM, Johnson AD, Kaplan R, Kardina
584 SLR, Kelly T, Kelly S, Kenny EE, Kiel DP, Klemmer R, Konkole BA, Kooperberg C, Kottgen A, Lange LA, Lasky-
585 Su J, Levy D, Lin X, Lin KH, Liu C, Loos RJF, Garman L, Gerszten R, Lubitz SA, Lunetta KL, Mak ACY,
586 Manichaikul A, Manning AK, Mathias RA, McManus DD, McGarvey ST, Meigs JB, Meyers DA, Mikulla JL,
587 Minear MA, Mitchell BD, Mohanty S, Montasser ME, Montgomery C, Morrison AC, Murabito JM, Natale
588 A, Natarajan P, Nelson SC, North KE, O'Connell JR, Palmer ND, Pankratz N, Peloso GM, Peyser PA,
589 Pleiness J, Post WS, Psaty BM, Rao DC, Redline S, Reiner AP, Roden D, Rotter JI, Ruczinski I, Sarnowski C,
590 Schoenherr S, Schwartz DA, Seo JS, Seshadri S, Sheehan VA, Sheu WH, Shoemaker MB, Smith NL, Smith
591 JA, Sotoodehnia N, Stilp AM, Tang W, Taylor KD, Telen M, Thornton TA, Tracy RP, Van Den Berg DJ,
592 Vasani RS, Viaud-Martinez KA, Vrieze S, Weeks DE, Weir BS, Weiss ST, Weng LC, Willer CJ, Zhang Y, Zhao
593 X, Arnett DK, Ashley-Koch AE, Barnes KC, Boerwinkle E, Gabriel S, Gibbs R, Rice KM, Rich SS, Silverman
594 EK, Qasba P, Gan W, Consortium NT-OfPM, Papanicolaou GJ, Nickerson DA, Browning SR, Zody MC,
595 Zollner S, Wilson JG, Cupples LA, Laurie CC, Jaquish CE, Hernandez RD, O'Connor TD and Abecasis GR.
596 Sequencing of 53,831 diverse genomes from the NHLBI TOPMed Program. *Nature*. 2021;590:290-299.
597 41. Crossfield SSR, Chaddock NJM, Iles MM, Pujades-Rodriguez M and Morgan AW. Interplay
598 between demographic, clinical and polygenic risk factors for severe COVID-19. *Int J Epidemiol*.
599 2022;51:1384-1395.

600 42. McCarthy S, Das S, Kretzschmar W, Delaneau O, Wood AR, Teumer A, Kang HM, Fuchsberger C,
601 Danecek P, Sharp K, Luo Y, Sidore C, Kwong A, Timpson N, Koskinen S, Vrieze S, Scott LJ, Zhang H,
602 Mahajan A, Veldink J, Peters U, Pato C, van Duijn CM, Gillies CE, Gandin I, Mezzavilla M, Gilly A, Cocca M,
603 Traglia M, Angius A, Barrett JC, Boomsma D, Branham K, Breen G, Brummett CM, Busonero F, Campbell
604 H, Chan A, Chen S, Chew E, Collins FS, Corbin LJ, Smith GD, Dedoussis G, Dorr M, Farmaki AE, Ferrucci L,
605 Forer L, Fraser RM, Gabriel S, Levy S, Groop L, Harrison T, Hattersley A, Holmen OL, Hveem K, Kretzler M,
606 Lee JC, McGue M, Meitinger T, Melzer D, Min JL, Mohlke KL, Vincent JB, Nauck M, Nickerson D, Palotie A,
607 Pato M, Pirastu N, McInnis M, Richards JB, Sala C, Salomaa V, Schlessinger D, Schoenherr S, Slagboom
608 PE, Small K, Spector T, Stambolian D, Tuke M, Tuomilehto J, Van den Berg LH, Van Rheenen W, Volker U,
609 Wijmenga C, Toniolo D, Zeggini E, Gasparini P, Sampson MG, Wilson JF, Frayling T, de Bakker PI, Swertz
610 MA, McCarroll S, Kooperberg C, Dekker A, Altshuler D, Willer C, Iacono W, Ripatti S, Soranzo N, Walter K,
611 Swaroop A, Cucca F, Anderson CA, Myers RM, Boehnke M, McCarthy MI, Durbin R and Consortium HR. A
612 reference panel of 64,976 haplotypes for genotype imputation. *Nat Genet*. 2016;48:1279-83.

613 43. Auton A, Brooks LD, Durbin RM, Garrison EP, Kang HM, Korbel JO, Marchini JL, McCarthy S,
614 McVean GA, Abecasis GR and Consortium GP. A global reference for human genetic variation. *Nature*.
615 2015;526:68-74.

616 44. Walter K, Min JL, Huang J, Crooks L, Memari Y, McCarthy S, Perry JR, Xu C, Futema M, Lawson D,
617 Iotchkova V, Schiffels S, Hendricks AE, Danecek P, Li R, Floyd J, Wain LV, Barroso I, Humphries SE, Hurles
618 ME, Zeggini E, Barrett JC, Plagnol V, Richards JB, Greenwood CM, Timpson NJ, Durbin R, Soranzo N and
619 Consortium UK. The UK10K project identifies rare variants in health and disease. *Nature*. 2015;526:82-
620 90.

621 45. Rohloff JC, Gelinis AD, Jarvis TC, Ochsner UA, Schneider DJ, Gold L and Janjic N. Nucleic Acid
622 Ligands With Protein-like Side Chains: Modified Aptamers and Their Use as Diagnostic and Therapeutic
623 Agents. *Mol Ther Nucleic Acids*. 2014;3:e201.

624 46. Di Angelantonio E, Thompson SG, Kaptoge S, Moore C, Walker M, Armitage J, Ouwehand WH,
625 Roberts DJ, Danesh J and Group IT. Efficiency and safety of varying the frequency of whole blood
626 donation (INTERVAL): a randomised trial of 45 000 donors. *Lancet*. 2017;390:2360-2371.

627 47. McLaren W, et al. The ensembl variant effect predictor. *Genome biology*. 2016;17:1-14.
628 48. MacArthur J, Bowler E, Cerezo M, Gil L, Hall P, Hastings E, Junkins H, McMahon A, Milano A,
629 Morales J, Pendlington ZM, Welter D, Burdett T, Hindorff L, Flicek P, Cunningham F and Parkinson H. The
630 new NHGRI-EBI Catalog of published genome-wide association studies (GWAS Catalog). *Nucleic Acids*
631 *Res*. 2017;45:D896-D901.
632 49. Kamat MA, Blackshaw JA, Young R, Surendran P, Burgess S, Danesh J, Butterworth AS and Staley
633 JR. PhenoScanner V2: an expanded tool for searching human genotype-phenotype associations.
634 *Bioinformatics*. 2019;35:4851-4853.
635 50. Hemani G, Zheng J, Elsworth B, Wade KH, Haberland V, Baird D, Laurin C, Burgess S, Bowden J,
636 Langdon R, Tan VY, Yarmolinsky J, Shihab HA, Timpson NJ, Evans DM, Relton C, Martin RM, Davey Smith
637 G, Gaunt TR and Haycock PC. The MR-Base platform supports systematic causal inference across the
638 human phenome. *Elife*. 2018;7.
639

Tables

Table 1. Best-fit polygenic risk scores for the 12 proteins with a PRS association P -value < 0.05 .

Protein Name	Gene Symbol	P_T^{\pm}	Developed PRS			Replication PRS			N (replication N)
			PRS R^2+	Coefficient (SE) [†]	P - value [†]	PRS R^2 ‡	Coefficient (SE)‡	P -value‡	
Apolipoprotein L1*	APOL1*	1.7×10^{-3}	0.00	-53.36 (10.03)	1×10^{-4}	0.002	-27.43 (8.23)	8.69×10^{-4}	2,278 (2261)
Interleukin 1 receptor, type II	IL1R2	3×10^{-4}	0.00	15.29 (3.97)	2.6×10^{-3}	1.26×10^{-4}	2.78 (3.15)	0.38	487 (477)
Superoxidase dismutase	SOD3	2.5×10^{-4}	0.00	15.36 (4.02)	4.2×10^{-3}	1.8×10^{-4}	3.37 (3.18)	0.29	388 (377)
C-C motif chemokine 22	CCL22	1.5×10^{-4}	0.00	10.04 (2.89)	0.01	4.58×10^{-5}	1.27 (2.38)	0.59	254 (252)
Coagulation factor X	F10	0.19	0.00	366.13 (106.2)	0.01	4.95×10^{-5}	-46.26 (83.43)	0.58	114,475 (110,963)

C1 inhibitor	SERPING	0.23	0.00	382.35	0.01	8.25 x	-0.64	0.99	130,831
	1		3	(112.25)		10 ⁻⁹	(89.50)		(126,859)
Plasminogen	PLG	5 x 10 ⁻⁸	0.00	0.83 (0.25)	0.01	0.019	-2.25 (0.20)	1.62 x 10 ⁻	11 (11)
			3					28	
Gastrin Releasing Peptide	GRP	5x 10 ⁻⁸	0.00	-0.49 (0.15)	0.02	4.05 x	-0.19 (0.12)	0.11	2 (2)
			3			10 ⁻⁴			
Complement C1q tumor necrosis factor-related protein 1	C1QTNF1	0.14	0.00	294.32	0.02	9.09 x	-52.33	0.45	91,757 (88,829)
			3	(90.47)		10 ⁻⁵	(69.64)		
Vitronectin	VTN	8.75 x	0.00	-72 (22.46)	0.02	0.001	-46.42	7.07 x 10 ⁻³	9,792 (9,544)
		10 ⁻³	3				(17.23)		
TNF-related weak inducer of apoptosis	TNFSF12	1.55 x	0.00	-30.48 (10.1)	0.04	3.14 x	-3.58 (0.66)	0.66	2,099 (2,042)
		10 ⁻³	3			10 ⁻⁵			
Melanoma-derived growth regulatory protein	MIA	0.02	0.00	90.59 (31.03)	0.05	2.06 x	9.09	0.72	16,226 (15,752)
			3			10 ⁻⁵	(25.38)		

*Best-fit PRS had a P-value which passes the Bonferroni-corrected threshold ($P\text{-value} \leq 2.96 \times 10^{-4}$).

†Statistic(s) relating to PRS developed in discovery phase.

‡Statistic(s) relating to replication stage PRS.

PRS, polygenic risk score; P_T , *P*-value threshold; R^2 , (Nagelkerke's pseudo R^2), variance in GCA risk explained by the risk score;

Coefficient, regression coefficient of the protein risk score association with GCA risk; *SE*, standard error; *N*, number of SNPs in risk score.

Table 2. Results of the Multi-marker Analysis of GenoMic Annotation (MAGMA) gene-based test, performed using SNPs of the apolipoprotein L1 PRS.

Gene Symbol	Encoded Protein	Chr	SNPs <i>N</i>	<i>Z</i>	<i>P</i>
<i>DNMBP</i>	Dynamin Binding Protein	10	590	8.3369	3.81 x 10 ⁻¹⁷
<i>LRRC15</i>	Leucine Rich Repeat Containing 15	3	113	7.7451	4.77 x 10 ⁻¹⁵
<i>CPN2</i>	Carboxypeptidase N Subunit 2	3	80	6.1094	5.00 x 10 ⁻¹⁰
<i>CPN1</i>	Carboxypeptidase N Subunit 1	10	154	6.1094	5.00 x 10 ⁻¹⁰
<i>CLPTM1</i>	Cleft lip and palate transmembrane protein 1	19	140	6.1038	5.18 x 10 ⁻¹⁰
<i>SLC46A1</i>	Proton-coupled folate transporter	17	20	5.3177	5.26 x 10 ⁻⁸
<i>BLOC1S2</i>	Biogenesis of lysosome-related organelles complex 1 subunit 2	10	48	5.2006	9.93 x 10 ⁻⁸
<i>APOC4</i>	Apolipoprotein C-IV	19	32	4.9299	4.11 x 10 ⁻⁷
<i>APOC4-</i>	Apolipoprotein C-	19	32	4.9299	4.11 x 10 ⁻⁷
<i>APOC2</i>	IV/Apolipoprotein C-II				
<i>POLDIP2</i>	Polymerase delta-interacting protein 2	17	17	4.769	9.26 x 10 ⁻⁷
<i>TNFAIP1</i>	BTB/POZ domain-containing protein	17	21	4.7196	1.18 x 10 ⁻⁶

<i>CTB-96E2.2</i>	-	17	14	4.6054	2.06×10^{-6}
<i>SARM1</i>	Sterile Alpha And TIR Motif Containing 1	17	103	4.5917	2.20×10^{-6}
<i>ERLIN1</i>	ER Lipid Raft Associated 1	10	100	4.5843	2.28×10^{-6}

SNP, single nucleotide polymorphism; *PRS*, polygenic risk score; *Chr*, chromosome; *N*, number;

Z, z-stat; *P*, P-value.

Figures

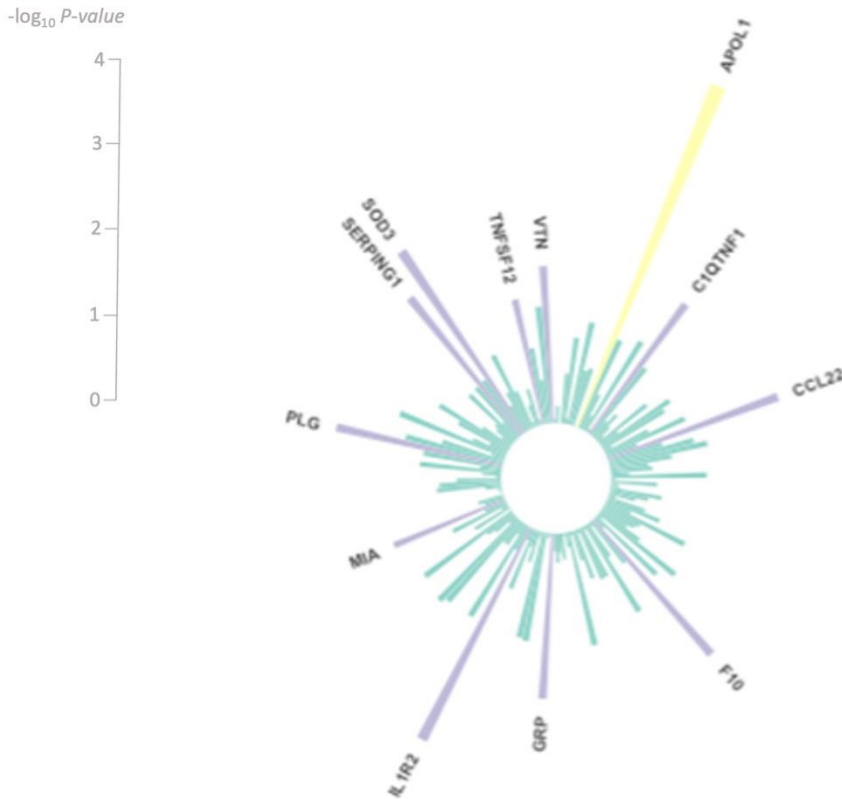


Figure 1. Circos plot of the $-\log_{10} P$ -values for association between the “best fit” polygenic risk scores (generated using protein quantitative trait loci (pQTL) summary statistics for each protein) and giant cell arteritis (GCA) case-control status. A significant association indicates that a single polygenic risk score for abundance of a particular protein also predicted GCA risk; the P -value (P) of this association is represented by the length of bar on the plot. These scores indicate shared genetic aetiology between the traits and are suggestive of a causal link between the protein levels and disease outcome. Blue bars represent associations not reaching the $P \leq 0.05$ threshold. Purple bars represent associations significant at $P \leq 0.05$ but which did not pass the Bonferroni-corrected $P \leq 2.96 \times 10^{-4}$ threshold. Yellow bars represent associations at the $P \leq 2.96 \times 10^{-4}$ Bonferroni-corrected threshold.

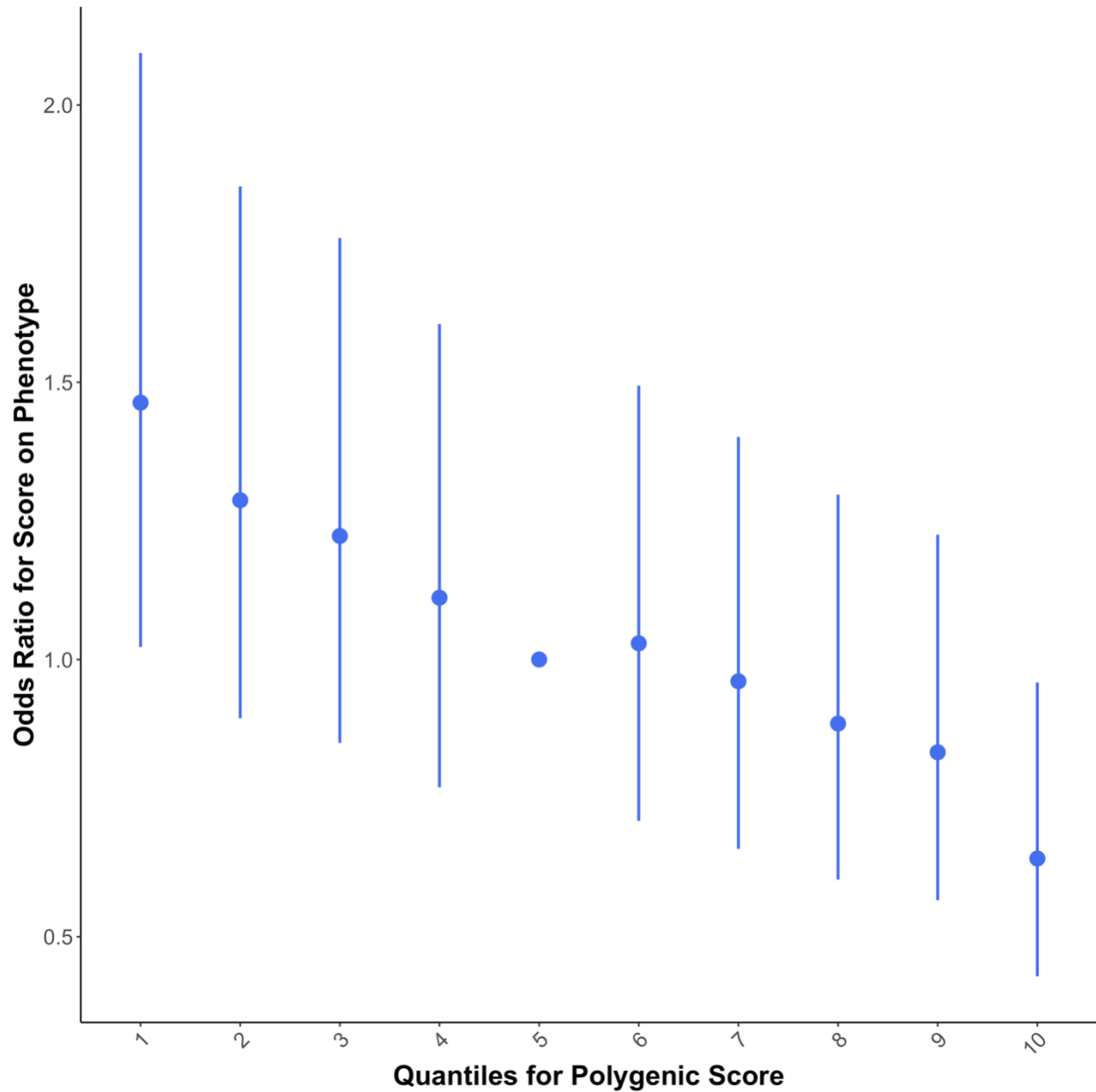


Figure 2. Quantile plot demonstrating the effect of increasing the optimal polygenic risk score (PRS) from Apolipoprotein L1 (APOL1) protein quantitative trait loci (pQTL) on giant cell arteritis (GCA) risk. Samples were assigned to a non-overlapping decile based on their PRS, and logistic regression was performed to generate odds ratios for the association between the APOL1 PRS decile and GCA risk. The fifth quantile is the reference and error

bars around points represent 95% confidence intervals. Increasing the APOL1 PRS value is associated with increased plasma levels of APOL1 and a decreased risk of GCA.

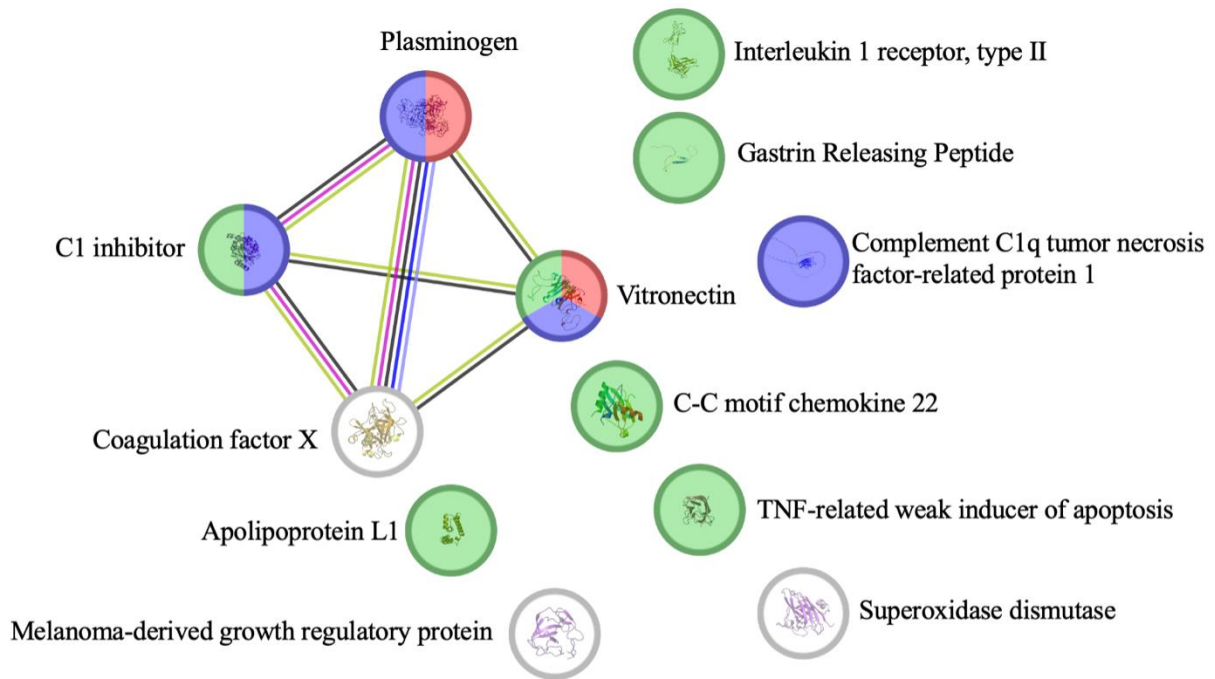


Figure 3. StringDB network analysis using proteins (nodes) whose PRS had “borderline” significant ($P\text{-value}\leq 0.05$) associations with GCA susceptibility. Nodes are coloured according to presence in enriched gene ontology biological pathways, including: “negative regulation of fibrinolysis” (red), “negative regulation of blood coagulation” (blue) and “immune response” (green). Edges of this network represent protein-protein links found by StringDB via textmining (green), coexpression (black), protein homology (light blue), gene co-occurrence (navy), and experimental (pink) evidence.

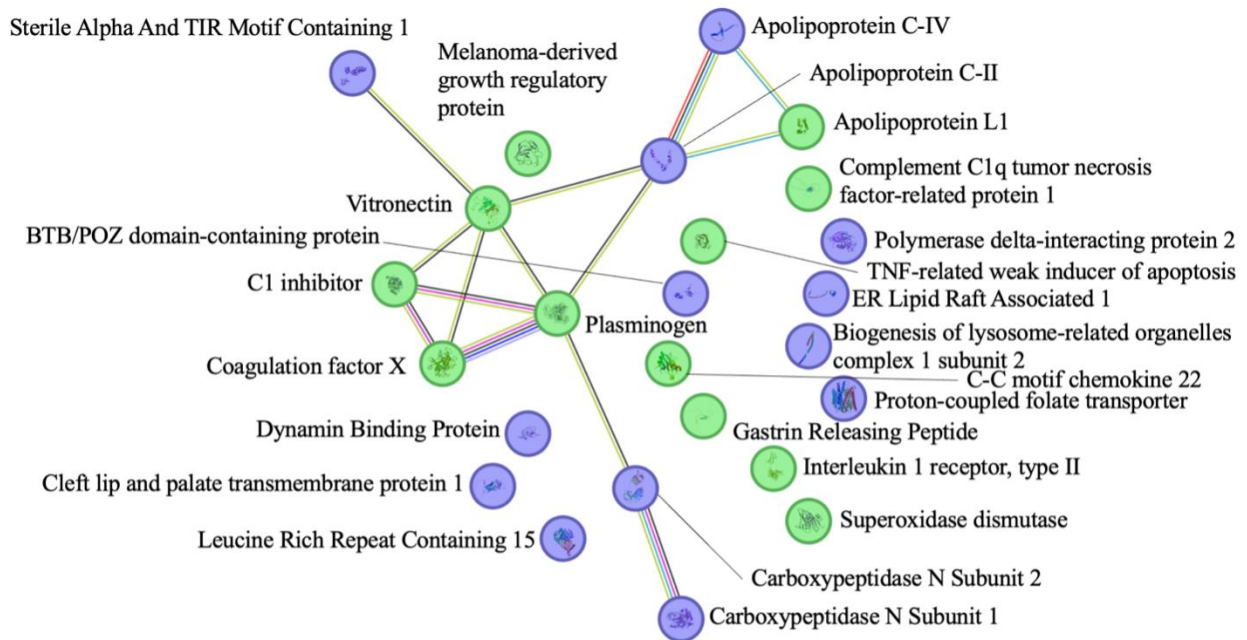


Figure 4. StringDB network analysis using proteins (nodes) whose PRS had “borderline” significant ($P\text{-value}\leq 0.05$) associations with GCA susceptibility (green nodes), or whose respective genes were enriched for SNPs in the APOL1 PRS (blue nodes). Edges of this network represent protein-protein links found by StringDB via textmining (green), coexpression (black), protein homology (light blue), gene co-occurrence (navy), experimental (pink), and gene fusion (red) evidence.

Supplementary Material

Supplementary Methods

Quality control of giant cell arteritis datasets

A case-control cohort comprised of samples from the UK giant cell arteritis (GCA) consortium ($N=1,858$) and the Wellcome Trust Case-Control Consortium (WTCCC; $N=3,748$) was used to optimize polygenic risk scores (PRS) in this work. Informed written consent was gained from all participants (Yorkshire and the Humber Leeds West Research Ethics Committee [05/Q1108/28]), including 1,858 cases with a confirmed clinical (consultant rheumatologist or ophthalmologist) diagnosis of GCA (i.e. biopsy confirmed, positive imaging or adequate symptomatic characteristics to allow for a sound clinical diagnosis). Of these individuals, 963/1,386 (69.48%) had a confirmed diagnosis (temporal artery biopsy [TAB] or imaging, including: magnetic resonance angiography [MRA], positron emission computed tomography with 2-deoxy-2-fluorine-18-fluoro-D-glucose [^{18}F FDG-PET/CT], ultrasound scan [USS], computed tomography [CT], and CT angiography [CTA]). Additionally, 1,287/1,379 cases (93.32%) fulfilled imputed American College of Rheumatology classification criteria⁹, including at least three of: new headache, age at disease onset ≥ 50 years, abnormal TAB, temporal artery abnormality, and heightened ESR (≥ 50 mm/hr). In this work, ESR was imputed from CRP, due to a lack of routine ESR measurements at several UK NHS sites at the time of data collection. For cases with both ESR and CRP available ($N=1001$), missing variable percentile analysis was performed, and it was found that for an ESR ≥ 50 mm/hr, the equivalent CRP measurement was 36mg/L (9th percentile). Therefore, for cases with missing ESR values, CRP measurements ≥ 36 mg/L were used to impute ESR ≥ 50 mm/hr (elevated ESR).

Three ischaemic phenotypes were defined in this cohort. Cranial ischaemic complications in GCA were defined as: non-ocular cranial complications such as tongue necrosis, scalp necrosis, or cerebrovascular accident at presentation (secondary to GCA); and ocular complications such as cranial nerve palsy (III, IV, or V), branch retinal artery occlusion, central retinal artery occlusion, cilioretinal artery occlusion, posterior ischaemic optic neuropathy, Anterior ischaemic optic neuropathy, irreversible visual loss, irreversible visual field defect, irreversible ocular motility, irreversible diplopia, or relative afferent pupillary defect. Transient cranial ischaemic manifestations were defined as: non-ocular cranial ischaemic features such as transient ischaemic attack at presentation (secondary to GCA), tongue claudication, or jaw claudication; and ocular ischaemic features such as transient vision loss, transient double vision/absence of ocular motility, transient reduced acuity, transient field defect or transient diplopia. Furthermore, non-cranial ischaemic manifestations were defined as: extra-cranial complications such as fixed vascular stenosis to limb at presentation (secondary to GCA); and extra-cranial ischaemic features such as leg claudication or arm claudication.

Details of the quality control (QC) of GCA case genetic data used for PRS optimization in this work has previously been described in Carmona et al. (2017). Briefly, deoxyribonucleic acid (DNA) was sequenced for UK GCA Consortium samples in three batches. For the first two batches (batch 1 $N=477$, batch 2 $N=239$, of 1,858 total) of genomic DNA were extracted from peripheral blood cells of subjects and genotyped using the Illumina “Infinium HumanCore Beadchip” and the Genotyping Module (v.1.9) of the GenomeStudio software (Illumina).⁷ For these two batches, plus the first batch of WTCCC samples (1958 British birth cohort), several variant QC filters were applied to the data in PLINK v1.07.,¹⁶ removing single nucleotide polymorphisms (SNPs) with call rates < 0.98 , minor allele frequency (MAF) < 0.01 , and variants

that deviated from Hardy-Weinberg equilibrium (HWE) at $P < 10^{-10}$ (for cases) or $P < 10^{-6}$ (for controls). Sex chromosomes were also removed from analyses. Sample QC removed individuals with a sample missingness rate $> 5\%$, and one of each pair of first-degree relatives (identity by descent [IBD] > 0.4) was removed. Principal component analysis (PCA) was performed in PLINK v.1.09.¹⁶ to account for population stratification in subsequent analyses. Imputation was performed using Minimac4 through the Michigan imputation server³⁹. Following imputation, further variant filters were applied, including removal of SNPs with MAF < 0.01 and with imputation quality $r^2 < 0.5$.

An additional 1,142 samples (batch 3) were later recruited to the UK GCA Consortium and genotyped using the Illumina Infinium “Global Screening Array”. For this batch, plus the second WTCCC sample cohort (UK blood service control group), sex chromosomes were removed from analyses and several variant QC filters were applied to the data in PLINK v1.09, removing SNPs with call rates < 0.98 , MAF < 0.002 , and variants that deviated from the Hardy-Weinberg equilibrium (HWE) at $P < 10^{-10}$ (for cases) or $P < 10^{-6}$ (for controls). Sample QC removed individuals with a sample missingness rate $> 3\%$, those who deviated > 3 standard deviations from the heterozygosity rate mean, and all samples with $\hat{p} > 0.2$ were removed following linkage disequilibrium (LD) based pruning (high inversion rate regions removed, *window size* [bp] = 50, *window shift* [SNPs] = 5, *LD* $R^2 = 0.2$). Principal component analysis (PCA) was performed in PLINK v.1.09. to account for population stratification in subsequent analyses. Imputation was performed using TopMed.⁴⁰

Quality control of UK Biobank genetic data

A comprehensive description of the QC of UK Biobank (UKB) genetic data used in this study may be found in Crossfield et al. (2022)⁴¹ and Bycroft et al. (2018)¹⁹. Briefly, participants were

genotyped using either the Affymetrix UK BiLEVE Axiom or Affymetrix UK Biobank Axiom array and imputation was performed using combined reference panels from the Haplotype Reference Consortium⁴², 1000 Genomes⁴³, and UK10K projects.⁴⁴ Sample filters included the removal of individuals above the heterozygosity rate mean of 0.19, high missingness rates (>5%), mismatching genetic/reported sex, and one sample from each pair of those estimated to be second-degree relatives or closer (preferentially removing that with the greater genotype missingness rate). Post imputation QC filters included the removal of samples with $MAF < 0.001$ and imputation quality $r^2 < 0.8$.

Following PCA, the “aberrant” routine in R was employed to detect ethnic outliers (non-Europeans) in PCs 1 and 2, using a lambda parameter of 100. Participants who i) fell within the European PC cluster and ii) self-reported “White” in UKB baseline data (field 21000) were retained for analysis, increasing the “white European” cohort size compared with UKB’s definition, which excludes samples who self-report as “Irish” or “any other white background”.

Protein selection

Proteins were selected for study in this work from publicly available summary statistics generated from GWAS investigating inter-individual variation of protein levels.¹³ These analyses were performed using protein quantification data from the multiplexed SOMAscan platform,⁴⁵ consisting of 3,283 modified aptamers (single stranded DNA SOMAmer reagents) for 2,994 proteins/protein complexes (post QC). Details of population demographics, genotyping, protein profiling, QC and statistical analyses of these GWAS have previously been described.¹³ Briefly, informed consent was provided by healthy participants of the INTERVAL study,⁴⁶ which consisted of two non-overlapping sub-cohorts of blood donors aged ≥ 18 ($N= 2,731$ and 831). The Affymetrix Axiom UK Biobank genotyping array was used to genotype participants and

imputation was performed using the Sanger imputation server, using a combined 1000 Genomes Phase 3-UK10K reference panel.

In order to prioritise the proteins investigated and minimise multiple testing, two filters were applied to the selection of plasma proteins for inclusion in the study. Firstly, 730 proteins deemed part of the “human blood secretome” were selected, based on prior knowledge that circulating proteins represent useful druggable targets and because their primary physiological action is in circulating form¹⁵. Secondly, proteins with low levels of heritability, and therefore unlikely to demonstrate strong genetic associations with GCA-risk, were removed from the study. Heritability (R^2) estimates (in the form of proportion of variance explained by genome-wide significant variants) were yielded from Sun et al. (2017),¹³ and only those proteins with heritability values greater than or equal to the lowest quartile R^2 estimate for the group were included in further analyses. After the removal of variants with a low heritability level, 169 proteins remained for analysis.

Polygenic risk scoring

The PRSice v2.3.3¹⁷ software was used for optimizing PRS and testing for associations with GCA. PRS were constructed via the “clumping and thresholding” approach, using effect sizes and *P-values* from GWAS of protein levels.¹³ SNPs were thinned in 500kb blocks, based on an LD R^2 threshold of 0.1. All SNPs beneath a specified *P-value* threshold (P_T) in the protein summary statistics were used to form a risk score, which was regressed on the GCA dataset, using the top 10 PCs from PCA as covariates. This process was repeated for risk scores at many P_T (minimum $P_T = 5 \times 10^{-8}$; step size = 5×10^{-5} ; maximum $P_T = 1$). The “best fit” risk score was defined as the PRS with the greatest GCA model fit (R^2) in logistic regression.

A permutation test was used to account for multiple testing within each analysis. This was conducted with PRSice v2.3.3¹⁷ using the following steps: (1) a “best-fit” risk score was generated; (2) the phenotype was randomly shuffled, the analysis was repeated and another “best-fit” score was generated; (3) step 2 was repeated 10,000 times; and (4) the empirical *p-value* was calculated as

$$\text{Empirical } - P = \frac{\sum_{n=1}^N I(P_{null} \geq P_0) + 1}{N + 1}$$

where $I(\cdot)$ is the indicator function, P_0 is the best-fit P_T and N is the number of times the analysis was repeated.

To account for multiple testing of numerous proteins, the significance threshold was adjusted using Bonferroni correction. For the 169 proteins assessed by PRS analysis, the corrected *P-value* threshold was $0.05/169 = 2.96 \times 10^{-4}$.

For proteins with a statistically significant PRS, risk scoring was repeated in high-resolution (using a smaller step size between each P_T tested; P_T step size= 5×10^{-8} as opposed to 5×10^{-5}), to increase the precision of the PRS. Variants of the risk score were classed as *cis*-pQTL if they were located within 1MB of the transcription start site of the gene encoding the protein; whilst variants located outside of this region were classed as *trans*-pQTL.

Polygenic Risk Score Analysis Using Different Case Definitions

To determine whether there was a difference in the average PRS between those with a “confirmed” GCA diagnosis (via imaging or biopsy) or fulfilling American College of Rheumatology [ACR] classification criteria (with an ACR score ≥ 3) and those without, a t-test was performed to assess whether there was a significant difference between the mean PRS at the

best fit P_T ($P_T = 1.66 \times 10^{-3}$) in a case-control approach (**Supplementary Table 1**). All individuals in this cohort had a clinical diagnosis of GCA.

Supplementary Table 1. Features of groups compared in PRS sensitivity analyses.

	Cases N	Controls N
Biopsy and/or imaging positive vs. Biopsy and imaging negative*	963	423
ACR score ≥ 3 vs. ACR score < 3†	1,287	92

N , number; ACR, American college of rheumatology.

*Individuals without diagnostic tests performed were excluded from this analysis.

†Individuals without documented ACR criteria/scores were excluded from this analysis.

To reduce bias from differences in the sample sizes of the groups, a permutation test was applied. A t-test was performed on the target phenotype to retrieve a test statistic. Phenotype values were then randomly re-assigned and a t-test performed again. This was repeated 10,000 times, creating an empirical distribution of the test statistic under the null hypothesis. Finally, an empirical P -value was calculated as:

$$\text{Empirical } - P = 1 - \frac{\sum_{n=1}^N I(F_0 \geq F_1)}{N}$$

Where $I(.)$ is the indicator function, F_0 is the F -value using the random sample, F_1 is the F -value using the initial sub-sample and N is the number of times the analysis was repeated.

Testing PRS associations with giant cell arteritis severity

To determine whether PRS associated with GCA susceptibility were also predictive of GCA severity, PRS which had a statistically significant association with GCA at the Bonferroni-

corrected threshold ($P\text{-value}=2.96 \times 10^{-4}$) were tested for association with a proxy for GCA severity: cranial ischaemic complications in GCA. This was performed in the GCA cohort with detailed clinical data available, with cases defined as GCA patients with reported cranial ischaemic complications and controls defined as GCA patients without reported cranial ischaemic complications (cases $N=317$, controls $N=1,542$). Two other proxies for disease severity were also used: transient cranial ischaemic manifestations in GCA (cases $N=1,127$, controls $N=719$), and non-cranial ischaemic features in GCA (cases $N=195$, controls $N=1,371$).

Mendelian randomization

To investigate the causality of associated proteins in GCA, case-control summary statistics (in the form of log odds ratios) were combined with summary statistics for associated proteins in MR.

Three genetic scores were constructed for use in MR, each with low levels of LD ($R^2 < 0.1$), and with RS numbers taken from Ensembl's Variant Effect Predictor (VEP)⁴⁷. The inverse-variance weighted (IVW) method was used to perform two-sample MR, and this was repeated using the weighted median and weighted mode methods. Sensitivity analyses (including Cochran's heterogeneity test and the MR-Egger intercept test) were performed on the scores to rule out potential horizontal pleiotropy, which could invalidate use of the genetic instruments¹⁴.

Potentially pleiotropic variants in MR sensitivity analyses were further investigated using a PheWAS approach. Genome-wide associations (defined as associations with a $p\text{-value} \leq 5 \times 10^{-8}$) were collated from three databases: GWAS Catalog⁴⁸, Phenoscanner⁴⁹, and the MR-Base PheWAS catalogue of summary data⁵⁰. Traits associated with ≥ 2 SNPs were used as the exposure variable in MR (using individual SNPs as genetic instruments with the Wald ratio

method), to test for a causal association between these traits and GCA via the SNPs in question. MR and sensitivity analyses were then repeated with outliers removed.

Supplementary Results

Polygenic risk scoring borderline significant results

A small number of protein PRS had associations with GCA which passed the $P < 0.05$ P -value threshold but not the Bonferroni-corrected threshold. These PRS were denoted “borderline” proteins in this work.

The interleukin 1 receptor type 2 (IL1R2) PRS had an association with GCA with a positive direction of effect (*coefficient*=15.29; *standard error*[SE]=3.97; *P-value*[P]= 2.6×10^{-3}). This PRS consisted of 487 SNPs ($P_T=3 \times 10^{-4}$) and had a model fit of $R^2=0.004$. Furthermore, a superoxide dismutase 3 (SOD3) PRS, consisting of 388 SNPs ($P_T=2.5 \times 10^{-4}$), had a GCA association with a positive direction of effect (*coefficient*=15.36; SE=4.03; $P=4.2 \times 10^{-3}$). This PRS had a model fit of $R^2=0.004$. The best-fit C-C motif chemokine ligand 22 (CCL22) PRS had an association with GCA with a positive direction of effect (*coefficient*=10.04; SE=2.89; $P=0.01$). This PRS had a model fit of $R^2=0.004$ and consisted of 254 SNPs ($P_T=1.5 \times 10^{-4}$). Additionally, a coagulation factor X (F10) PRS, comprising 114,475 SNPs ($P_T=0.19$) had an association with GCA with a positive direction of effect (*coefficient*=366.13; SE=106.2; $P=0.01$). This PRS had a model fit of $R^2=0.003$.

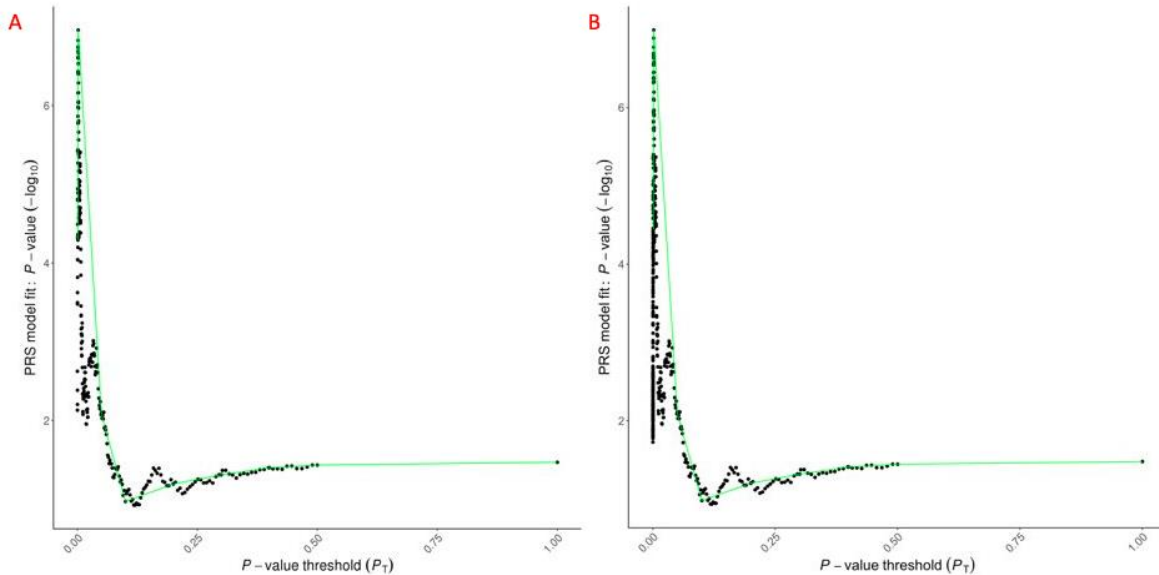
The serpin family G member 1 (SERPING1, otherwise known as C1-inhibitor) PRS had an association with GCA with a positive direction of effect (*coefficient*=382.35; SE=112.25; $P=0.01$). This PRS consisted of 130,831 SNPs ($P_T=0.23$) and had a model fit of $R^2=0.003$. The 11 SNP ($P_T=5 \times 10^{-8}$) plasminogen (PLG) PRS was associated with GCA, with a positive

direction of effect (coefficient=0.83; $SE=0.25$; $P=0.01$) and a model fit of $R^2=0.003$. Likewise, the gastrin-releasing peptide (GRP) PRS was also associated with GCA (coefficient=-0.49; $SE=0.15$; $P=0.02$). The 2 SNP PRS ($P_T=5 \times 10^{-8}$) had a model fit of $R^2=0.003$ and a negative direction of effect.

The C1Q and TNF related 1 (C1QTNF1) PRS was associated with GCA, with a positive direction of effect (coefficient=294.32; $SE=90.47$; $P=0.02$). This 91,757 SNP PRS ($P_T=0.14$) had a model fit of $R^2=0.003$. The vitronectin (VTN) PRS, comprised of 9,792 SNPs ($P_T=8.75 \times 10^{-3}$), had an association with GCA with a negative direction of effect (coefficient=-72; $SE=22.46$; $P=0.02$). This PRS had a model fit of $R^2=0.003$. Likewise, the 2,099 SNP ($P_T=1.55 \times 10^{-3}$) TNF superfamily member 12 (TNFSF12) PRS had a GCA association with a negative direction of effect (coefficient=-30.48; $SE=10.1$; $P=0.04$), with a model fit of $R^2=0.003$. Finally, the melanoma inhibitory activity (MIA) PRS, consisting of 16,226 SNPs, had an association with GCA with a positive direction of effect (coefficient=90.59; $SE=31.03$; $P=0.05$). This PRS had a model fit of $R^2=0.003$.

High-resolution APOL1 scoring

To increase the precision of the APOL1 risk score, risk scoring was performed at greater resolution, by reducing the step size between P -value thresholds (**Supplementary Figure 1**). Results revealed that the best-fit P_T was marginally smaller than that found in the first analysis and consisted of 51 fewer SNPs ($P_T=1.66 \times 10^{-3}$; $N=2,227$). Additionally, the regression coefficient of the relationship was more extreme (coefficient=-320.49, $SE=60.22$).



Supplementary Figure 1. Comparison of high-resolution plots generated in the regression of APOL1 risk scores on GCA-risk. Each plot shows significance values of the model fit ($-\log_{10} P\text{-values}$) between all polygenic risk scores (PRS) generated from Apolipoprotein L1 (APOL1) protein quantitative trait loci (pQTL) and risk of giant cell arteritis (GCA). The green line connects points demonstrating broad $P\text{-value}$ thresholds (P_T) displayed in the corresponding bar plots (see Figure 4.2). A) high-resolution plot generated using a P_T step size of 5×10^{-5} ; B) high-resolution plot generated using a P_T step size of 5×10^{-8} .

Polygenic Risk Score Analysis Using Different Case Definitions

To assess whether individuals with greater diagnostic confidence demonstrate a stronger genetic propensity to GCA through the APOL1 PRS, the case cohort was stratified based on the presence of a confirmed diagnosis, and the average PRS at the optimal P_T was compared.

No statistically significant difference in the APOL1 PRS was observed between those with a positive biopsy and/or imaging result, and those without a positive biopsy or imaging result ($t[785.55] = -0.23$, $P = 0.41$, positive biopsy/imaging mean = -0.08 , negative biopsy/imaging mean = -0.09). A similar observation was made when comparing those with an ACR score ≥ 3 and

those with an ACR score < 3 ($t[102.16]=0.1$, $P=0.54$, positive biopsy/imaging mean=-0.06; negative biopsy/imaging mean=-0.08).

Testing PRS associations with secondary outcomes

To determine whether those PRS associated with GCA susceptibility were also predictive of GCA severity, PRS were tested for associations with several ischaemic phenotypes in GCA, proxies for disease severity (**Supplementary Table 2**). The APOL1 PRS did not demonstrate a statistically significant association with cranial ischaemic complications (*odds ratio*[*OR*]=0.76, *95% confidence intervals*[*CI*s]=0.51 to 1.12, $P=0.324$, for the highest versus lowest APOL1 quintile), transient cranial ischaemic manifestations (*OR*[*95% CI*s]=1.15 [0.85 to 1.55], $P=0.53$, for the highest versus lowest APOL1 quintile), or non-cranial ischaemic features (*OR*[*95% CI*s]=1.15 [0.85 to 1.55], $P=0.53$, for the highest versus lowest APOL1 quintile).

Supplementary Table 2. APOL1 polygenic risk score associations with proxies for GCA severity, including: cranial ischaemic complications in GCA, transient cranial ischaemic manifestations in GCA, and non-cranial ischaemic features in GCA.

Outcome	APOL1 PRS quantile	OR (95%CI)	<i>P</i>	DF	Cases	Controls
Cranial ischaemic complications ¹						
	1	1	0.324	1,843	317	1,542
	2	0.98 (0.67 to 1.43)				
	3	0.83 (0.56 to 1.22)				
	4	1.06 (0.73 to 1.53)				
	5	0.76 (0.51 to 1.12)				
Transient cranial ischaemic manifestations ²						

1	1	0.533	1,831	1,127	719
2	1.12 (0.83 to 1.5)				
3	1.17 (0.87 to 1.57)				
4	1.01 (0.75 to 1.36)				
5	1.15 (0.85 to 1.55)				
Non-cranial ischaemic features ³					
1	1	0.129	1,553	195	1,371
2	0.81 (0.51 to 1.29)				
3	0.84 (0.53 to 1.33)				
4	0.77 (0.48 to 1.22)				
5	0.73 (0.46 to 1.16)				

APOLI PRS, apolipoprotein L1 polygenic risk score; OR, odds ratio; 95%CI, 95% confidence intervals; P, P-value

¹**Cranial ischaemic complications:** non-ocular cranial complications (tongue necrosis, scalp necrosis, cerebrovascular accident at presentation [secondary to GCA], ocular complications (cranial nerve palsy [III, IV, or V], branch retinal artery occlusion, central retinal artery occlusion, cilioretinal artery occlusion, posterior ischaemic optic neuropathy, Anterior ischaemic optic neuropathy, irreversible visual loss, irreversible visual field defect, irreversible ocular motility, irreversible diplopia, relative afferent pupillary defect).

²**Transient cranial ischaemic manifestations:** non-ocular cranial ischaemic features (transient ischaemic attack at presentation [secondary to GCA], tongue claudication, jaw claudication), ocular ischaemic features (transient vision loss, transient double vision/absence of ocular motility, transient reduced acuity, transient field defect, transient diplopia).

³**Non-cranial ischaemic manifestations:** extra-cranial complications (fixed vascular stenosis to limb at presentation [secondary to GCA]); extra-cranial ischaemic features (leg claudication, arm claudication).

Mendelian randomization

In MR, genetic variants are used as instrumental variables (IVs) to assess the causal relationship between an exposure (e.g. protein) and an outcome (e.g. GCA-risk). Three genetic scores were constructed for use as IVs in this study: a “liberal” score (APOL1 *P-value* $\leq 1 \times 10^{-4}$), an “intermediate” score (APOL1 *P-value* $\leq 5 \times 10^{-5}$), and a “conservative” score (APOL1 *P-value* $\leq 5 \times 10^{-8}$). A small number (n = 2) of variants were lost from the scores due to the inability of VEP to generate SNP RS numbers.

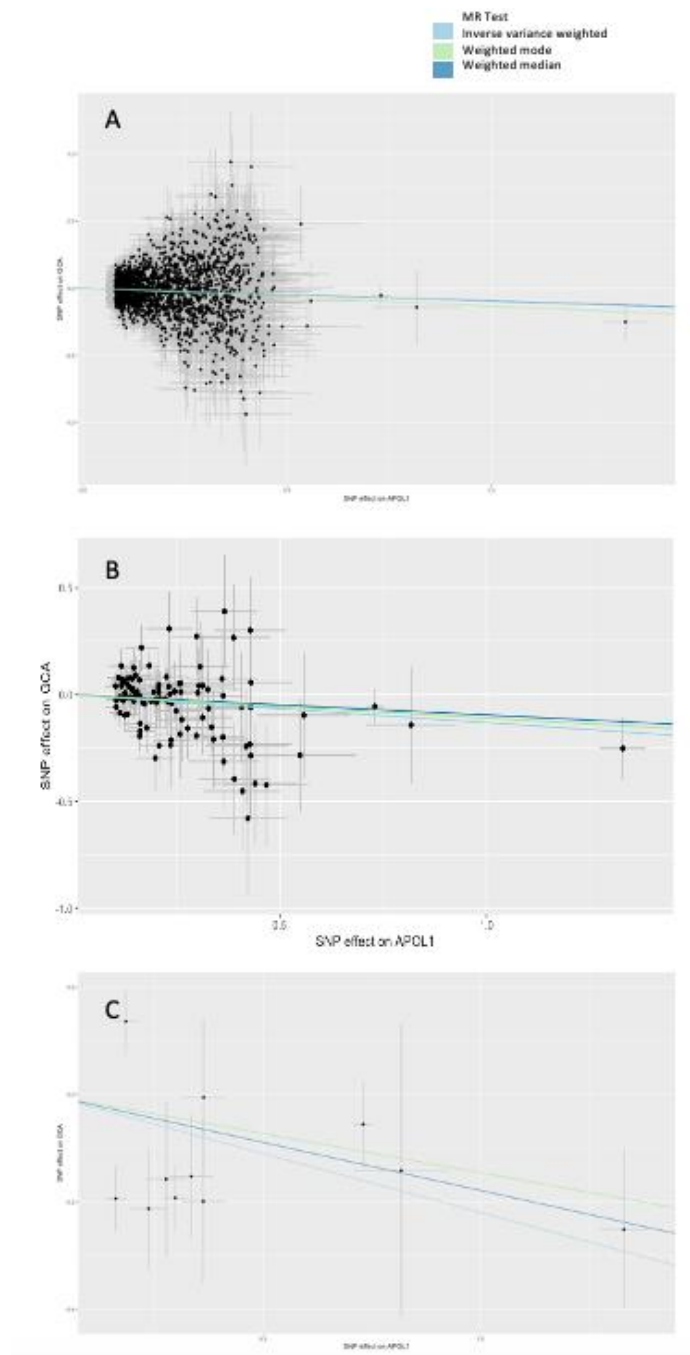
Once effect and non-effect alleles were harmonised between the exposure (pQTL) and outcome (GCA-risk) data, MR analysis was performed using each of the three risk scores. Using the IVW method of MR, the APOL1 protein was estimated by all risk scores to have a statistically significant, causal effect on GCA-risk (**Supplementary Table 3**). This direction of effect was always negative (liberal *beta*[*SE*]=-0.093[0.02]; intermediate *beta*[*SE*]=-0.131[0.05]; conservative *beta*[*SE*]=-0.22[0.1]), and was supported by the weighted median and weighted mode methods of MR (**Supplementary Figure 3**); although statistical significance was only found using the weighted median method with the liberal score, and the weighted mode method with the conservative score.

Supplementary Table 3. Causal estimation of the effect of Apolipoprotein L1 (APOL1) on giant cell arteritis (GCA) risk using various methods of performing mendelian randomization (MR).

Score	Method	SNPs <i>N</i>	<i>Beta</i>	<i>SE</i>	<i>P-value</i>
Liberal	IVW	2213	-0.093	0.02	4.42×10^{-9}
Liberal	Weighted median	2213	-0.096	0.03	4.46×10^{-3}
Liberal	Weighted mode	2213	-0.134	0.07	0.07
Intermediate	IVW	105	-0.131	0.05	3.6×10^{-3}
Intermediate	Weighted median	105	-0.095	0.07	0.16

Intermediate	Weighted mode	105	-0.11	0.08	0.17
Conservative	IVW	11	-0.22	0.1	0.03
Conservative	Weighted median	11	-0.15	0.08	0.09
Conservative	Weighted mode	11	-0.18	0.09	0.04

SNP, single nucleotide polymorphism



Supplementary Figure 3. Scatter plot of the per-SNP effect of the (top) liberal (1×10^{-4}), (middle) intermediate (5×10^{-5}), and (bottom) conservative ($P < 1 \times 10^{-4}$) Apolipoprotein L1 (APOL1) risk scores on giant cell arteritis (GCA) risk, with the causal estimates of the entire risk score regressed onto the plot and colour coded by method (inverse variance weighted, weighted median and weighted mode MR).

Results of the MR-Egger intercept test lacked statistical significance for any of the risk scores (**Supplementary Table 4**), indicating that directional horizontal pleiotropy of SNPs in the risk score is unlikely to have affected the effect size or direction of estimates. However, there was evidence for pleiotropy in the conservative score (Cochran's $Q=24.8$; *degrees of freedom*=10; *P-value*= 5.71×10^{-3}).

Supplementary Table 4. Summary of results from MR sensitivity analyses performed using the APOL1 PRS.

Risk Score	MR-Egger intercept (SE)	MR-Egger intercept <i>P-value</i>	Cochran's Q	Cochran's Q DF	Cochran's Q <i>P-value</i>
Liberal	-0.005 (0.005)	0.31	2209.1	2212	0.51
Intermediate	0.03 (0.017)	0.06	101.67	104	0.55
Conservative	-0.07 (0.07)	0.34	24.82	10	5.71×10^{-3}

SNPs from the conservative score ($N=11$) were investigated using a PheWAS in order to identify associations with other proteins that could be acting as alternate causal pathways to GCA.

PheWAS results revealed 19 proteins/traits that have a statistically significant association with two or more variants (**Supplementary Table 5**). These traits were used as exposure variables to assess their causal association with GCA in MR. 14 results (across 3 SNPs: rs11599750, rs5167

and rs704) revealed a statistically significant causal effect of the trait on GCA-risk, in the same direction as the variant's direct association with GCA-risk (**Supplementary Table 6**). These SNPs are located on different chromosomes (chromosomes 10, 19 and 17, respectively), so LD is unlikely to be affecting these associations. Such results provide evidence that these variants could be affecting GCA-risk through a pathway other than APOL1, and may therefore be inappropriate genetic instruments for use in APOL1 MR. It should be noted that when multiple testing correction is applied to these analyses using the Bonferroni method, none of the associations identified would have passed the $0.05/53 = 9.43 \times 10^{-4}$ *P-value* threshold.

Supplementary Table 5. Matrix summarising proteins/traits for which associations with SNPs of the conservative APOL1 PRS were identified.

Trait	rs11190387	rs113952349	rs114295003	rs11599750	rs17880383	rs182668035	rs61751507	rs1874125	rs5167	rs6809081
<i>HAAO</i>	Y		Y	Y			Y	Y		Y
<i>JAK2</i>	Y			Y						Y
<i>MMP8</i>		Y		Y			Y			
<i>CAST</i>				Y	Y		Y			
<i>PCDHA7</i>	Y	Y					Y			Y
<i>APOA</i>				Y					Y	
<i>CGREF1</i>	Y						Y			Y
<i>ALT</i>				Y	Y					
<i>AST</i>				Y	Y					
<i>GGT2</i>				Y	Y					
Triglycerides									Y	
<i>FKBP6</i>									Y	
<i>DEAF1</i>									Y	
<i>MAPKAPK5</i>									Y	
<i>LRTM2</i>									Y	
<i>USP21</i>									Y	
<i>APOB</i>									Y	
<i>GALP</i>									Y	
<i>IL27</i>				Y			Y			

SNP, single nucleotide polymorphism; APOL1, apolipoprotein-L1; PRS, polygenic risk score; HAAO, 3-Hydroxyanthranilate 3,4-dioxygenase; JAK2, Janus kinase 2; MMP8, matrix metalloproteinase-8; CAST, calpastatin; PHA7, protocadherin Alpha 7; GGT2, gamma-Glutamyltransferase 2; CGREF1, Cell Growth Regulator With EF-Hand Domain 1; FKBP6, FKBP Prolyl Isomerase Family Member 6; DEAF1, Deformed epidermal autoregulatory factor 1; MAPKAPK5, MAP kinase-activated protein kinase 5; LRTM2,

leucine rich repeats and transmembrane domains 2; USP21, Ubiquitin Specific Peptidase 21; APOB; apolipoprotein B; GALP, Galanin Like Peptide; APOA, apolipoprotein A; ALT, Alanine transaminase; AST, aspartate aminotransferase; IL27, interleukin 27.

Supplementary Table 6. Results of GCA susceptibility MR analyses using proteins/traits identified in PheWAS as exposure variables.

Trait	SNP	SNP-GCA <i>beta</i>	SNP-GCA <i>SE</i>	SNP-GCA <i>P</i> - <i>value</i>	Trait-GCA <i>beta</i>	Trait-GCA <i>SE</i>	Trait-GCA <i>P</i> - <i>value</i>	
HAAO	rs11190387	-0.21	0.11	0.06	-1.09	0.57	0.06	
	rs11429500	0.2	0.15	0.19	-0.49	0.38	0.19	
	3							
	rs11599750	0.19	0.06	1.8×10^{-3}	-0.79	0.25	1.8×10^{-3}	
	rs1874125	-0.16	0.14	0.27	-0.57	0.52	0.27	
	rs6809081	0.06	0.08	0.48	-0.08	0.11	0.48	
	rs704	-0.19	0.06	1.58×10^{-3}	-1.081	0.34	1.59×10^{-3}	
JAK2	rs61751507	0.25	0.15	0.09	-0.32	0.19	0.09	
	rs11190387	-0.21	0.11	0.06	-2.69	1.41	0.06	
	rs11599750	0.19	0.06	1.8×10^{-3}	-1.26	0.4	1.8×10^{-3}	
	rs6809081	0.05	0.08	0.48	-0.24	0.34	0.48	
		rs704	-0.19	0.06	1.57×10^{-3}	-0.5	0.16	1.59×10^{-3}
MMP8	rs11395234	0.15	0.12	0.19	-0.49	0.37	0.19	
	9							
	rs11599750	0.19	0.0	1.8×10^{-3}	-0.75	0.24	1.8×10^{-3}	
	rs704	-0.19	0.06	1.58×10^{-3}	0.9	0.29	1.59×10^{-3}	
CAST	rs61751507	0.25	0.15	0.09	-0.32	0.19	0.09	
	rs11599750	0.19	0.06	1.8×10^{-3}	-0.85	0.27	1.85×10^{-3}	
	rs17880383	5.82×10^{-3}	0.15	0.97	-0.02	0.48	0.97	
		rs704	-0.19	0.06	1.58×10^{-3}	1.38	0.44	1.56×10^{-3}
PCDHA7	rs61751507	0.25	0.15	0.09	-0.38	0.22	0.09	
	rs11190387	-0.21	0.11	0.06	11.26	5.91	0.06	
	rs11395234	0.15	0.12	0.19	0.38	0.29	0.19	
	9							
	rs6809081	0.06	0.08	0.48	-0.31	0.44	0.48	
GGT2	rs61751507	0.25	0.15	0.09	0.28	0.17	0.09	
		rs11599750	0.19	0.06	1.85×10^{-3}	137.75	44.14	1.8×10^{-3}
		rs17880383	5.81×10^{-3}	0.15	0.97	0.08	1.93	0.97
CGREF1	rs11190387	-0.21	0.11	0.06	-4.48	2.35	0.06	
	rs6809081	0.06	0.08	0.48	-0.23	0.33	0.48	
	rs61751507	0.25	0.15	0.09	-0.46	0.27	0.09	
FKBP6		rs5167	0.14	0.06	0.08	0.66	0.3	0.03
		rs704	-0.19	0.06	1.58×10^{-3}	-0.19	0.06	1.59×10^{-3}

DEAF1	<i>rs5167</i>	0.14	0.06	0.03	0.68	0.31	0.03
	rs704	-0.19	0.06	1.58×10^{-3}	-2.52	0.8	1.59×10^{-3}
MAPKAP K5	rs5167	0.14	0.06	0.03	-8.71	3.94	0.03
	rs704	-0.19	0.06	1.58×10^{-3}	3.74	1.18	1.59×10^{-3}
LRTM2	<i>rs5167</i>	0.14	0.06	0.03	0.73	0.33	0.03
	<i>rs704</i>	-0.19	0.06	1.58×10^{-3}	-4.51	1.423	1.59×10^{-3}
USP21	<i>rs5167</i>	0.14	0.06	0.03	0.27	0.12	0.03
	<i>rs704</i>	-0.19	0.06	1.58×10^{-3}	-2.24	0.71	1.59×10^{-3}
APOB	<i>rs5167</i>	0.14	0.06	0.03	4.98	2.25	0.03
	<i>rs704</i>	-0.19	0.06	1.58×10^{-3}	-69.38	21.96	1.59×10^{-3}
GALP	rs5167	0.14	0.06	0.03	-0.92	0.42	0.03
	rs704	-0.19	0.06	1.58×10^{-3}	1.3	0.41	1.59×10^{-3}
APOA	<i>rs11599750</i>	0.19	0.06	1.8×10^{-3}	13.34	4.27	1.8×10^{-3}
	<i>rs5167</i>	0.14	0.06	0.03	14.55	6.59	0.03
	rs704	-0.19	0.06	1.58×10^{-3}	9.95	3.15	1.56×10^{-3}
ALT	rs11599750	0.19	0.06	1.8×10^{-3}	-5.51	1.76	1.8×10^{-3}
	rs17880383	5.82×10^{-3}	0.15	0.97	-0.11	2.7	0.97
AST	rs11599750	0.19	0.06	1.8×10^{-3}	-6.68	2.14	1.8×10^{-3}
	rs17880383	5.82×10^{-3}	0.15	0.97	-0.13	3.23	0.97
Triglycerides	rs704	-0.19	0.06	1.58×10^{-3}	14.78	4.68	1.56×10^{-3}
	<i>rs5167</i>	0.14	0.06	0.03	9.99	4.52	0.03
IL27	rs11599750	0.19	0.06	1.8×10^{-3}	-1.21	0.39	1.8×10^{-3}
	rs61751507	0.25	0.15	0.09	-0.32	0.19	0.09

GCA, giant cell arteritis; MR, Mendelian randomization; PheWAS, phenome-wide association study; SNP, single nucleotide polymorphism; SE, standard error; HAAO, 3-Hydroxyanthranilate 3,4-dioxygenase; JAK2, Janus kinase 2; MMP8, matrix metalloproteinase-8; CAST, calpastatin; PHA7, protocadherin Alpha 7; GGT2, gamma-Glutamyltransferase 2; CGREF1, Cell Growth Regulator With EF-Hand Domain 1; FKBP6, FKBP Prolyl Isomerase Family Member 6; DEAF1, Deformed epidermal autoregulatory factor 1; MAPKAPK5, MAP kinase-activated protein kinase 5; LRTM2, leucine rich repeats and transmembrane domains 2; USP21, Ubiquitin Specific Peptidase 21; APOB, apolipoprotein B; GALP, Galanin Like Peptide; APOA, apolipoprotein A; ALT, Alanine transaminase; AST, aspartate aminotransferase; IL27, interleukin 27.

Once the three outliers (rs704, rs11599750 and rs5167) were removed, MR was repeated with each risk score. Using the IVW method of MR, the causal effect of the APOL1 protein on GCA risk remained statistically significant for each of the risk scores, with a negative direction of effect. Sensitivity analyses revealed that horizontal pleiotropy was now unlikely to be affecting the causal estimate (**Supplementary Table 7**).

Supplementary Table 7. Results of MR-Egger and Cochran’s *Q* sensitivity analyses using the conservative APOL1 PRS with rs704, rs11599750 and rs5167 removed.

Risk Score	MR-Egger intercept (SE)	MR-Egger intercept <i>P</i>-value	Cochran’s <i>Q</i>	Cochran’s <i>Q</i> DF	Cochran’s <i>Q</i> <i>P</i>-value
Liberal	-0.01 (0.004)	0.24	2187.22	2209	0.63
Intermediate	0.03 (0.02)	0.06	80.49	101	0.93
Conservative	-0.13 (0.09)	0.18	5.36	7	0.62

APOL1, apolipoprotein-L1; *PRS*, polygenic risk score; *SE*, standard error; *DF*, degrees of freedom.

UK GCA Consortium

Management Team: Ann W Morgan, Sarah L Mackie, Louise Sorensen

Laboratory Team: Lubna Haroon Raashid, Steve Martin, James I Robinson

School of Medicine, University of Leeds, Leeds UK

Recruiting Sites:

Chapel Allerton Hospital, Chapeltown Road, Leeds, LS7 4SA, UK

PI: Ann Morgan, Sarah Mackie

Research staff: Oliver Wordsworth, Isobel Whitwell, Jessica Brock

Pinderfields General Hospital, Aberford Road, *Wakefield*, WF1 4DG, UK

PI: Victoria Douglas, Chamila Hettiarachchi

Research staff: Jacqui Bartholomew

Dewsbury District and General Hospital, Halifax Road, Dewsbury, WF13 4HS, UK

PIs: Stephen Jarrett, Gayle Smithson, Chamila Hettiarachchi

Research staff: Jacqui Bartholomew

York Hospital, Wigginton Road, York, YO31 8HE, UK

PI: Michael Green

Research staff: Pearl Clark Brown

Harrogate District Hospital, Lancaster Park Rd, Harrogate, HG2 7SX, UK

PI: Cathy Lawson

Research staff: Esther Gordon

Ipswich Hospital, Heath Road, Ipswich, IP4 5PD, UK

PI: Suzanne Lane

Research staff: Rebecca Francis

Southend Hospital, Prittlewell Chase, Westcliff-on-Sea, Essex, SS0 0RY, UK

PI: Bhaskar Dasgupta, Bridgett Masunda

Research staff: Jo Calver

Hull Royal Infirmary, Anlaby Road, *Hull*, HU3 2JZ, UK

PI: Yusuf Patel

Research staff: Charlotte Thompson, Louise Gregory

Croydon University Hospital, 530 London Road, Croydon, Surrey, CR7 7YE, UK

PI: Sarah Levy

Haywood Hospital, High Lane, Burslem, Staffordshire, ST6 7AG, UK

PI: Ajit Menon

Research staff: Amy Thompson, Lisa Dyche, Michael Martin

Royal Surrey County Hospital, Egerton Road, Guildford, GU2 7XX, UK

PI: Charles Li

Queen's Hospital, Belvedere Road, Burton-on-Trent, DE13 0RB, UK

PI: Ramasharan Laxminarayan

Research staff: Louise Wilcox, Ralph de Guzman

Freeman Hospital, Freeman Road, High Heaton, Newcastle upon Tyne, Tyne and Wear, NE7 7DN, UK

PI: John Isaacs, Alice Lorenzi, Gary Reynolds

Research staff: Ross Farley, Helain Hinchcliffe-Hume

Barnsley Hospital, Gawber Road, Barnsley, S75 2EP, UK

PI: Victoria Bejarano

Research staff: Susan Hope

Northampton General Hospital, Cliftonville, Northampton, NN1 5BD, UK

PI: Pradip Nandi

Research staff: Lynne Stockham, Catherine Wilde, Donna Durrant

Frimley Park Hospital, Portsmouth Road, Camberley, GU16 7UJ, UK

PI: Mark Lloyd

Doncaster Royal Infirmary, Armthorpe Road, Doncaster, DN2 5LT, UK

PI: Chee-Seng Ye, Rob Stevens

Chelsea and Westminster Hospital, Fulham Road, London, SW10 9NH, UK

PI: Amjad Jilani

Great Western Hospital, Marlborough Road, Swindon, SN3 6BB, UK

PI: David Collins

Research staff: Suzannah Pegler, Ali Rivett, Liz Price

Royal National Hospital for Rheumatic Diseases, Upper Borough Walls, Bath, Avon, BA1 1RL, UK

PI: Neil McHugh, Sarah Skeoch

Research staff: Diana O'Kane, Sue Kirkwood

Gateshead Queen Elizabeth Hospital, Queen Elizabeth Avenue, Gateshead, NE9 6SX, UK

PI: Saravanan Vadivelu

Research staff: Susan Pugmire

Airedale General Hospital, Skipton Road, Keighley, BD20 6TB, UK

PI: Shabina Sultan

Research staff: Emma Dooks, Lisa Armstrong

Warrington Hospital, Lovely Lane, Warrington, Cheshire, WA5 1QG, UK

PI: Hala Sadik

Basildon University Hospital, Nethermayne, Basildon, SS16 5NL, UK

PI: Anupama Nandagudi

Research staff: Tolu Abioye, Angelo Ramos, Steph Gumus

St George's Hospital, Blackshaw Road, London, SW17 0QT, UK

PI: Nidhi Sofat

Research staff: Abiola Harrison, Abi Seward

Queen Elizabeth Hospital, Mindelsohn Way, Birmingham, B15 2TH, UK

PI: Susan Mollan

Research staff: Ray Rahan, Helen Hawkins

Royal Preston Hospital, Sharoe Green Lane, Preston, PR2 9HT, UK

PI: Hedley Emsley, Anna Bhargava

Research staff: Vicki Fleming, Marianne Hare, Sonia Raj

Arrowe Park Hospital, Arrowe Park Road, Birkenhead, CH49 5PE, UK

PI: Emmanuel George

Research staff: Nicola Allen, Karl Hunter

King's College Hospital, Denmark Hill, London, SE5 9RS, UK

PI: Eoin O'Sullivan

Research staff: Georgina Bird

Stoke Mandeville Hospital, Mandeville Road, Aylesbury, HP21 8AL, UK

PI: Malgorzata Magliano

Research staff: Katarina Manzo, Bobbie Sanghera

Royal Cornwall Hospital, Treliske, Truro, TR1 3LJ, UK

PI: David Hutchinson

Research staff: Fiona Hammonds

Peterborough City Hospital, Bretton Gate, Peterborough, PE3 9GZ, UK

PI: Poonam Sharma

Research staff: Richard Cooper, Graeme McLintock

Scarborough Hospital, Woodlands Drive, Scarborough, YO12 6QL, UK

PI: Zaid S. Al-Saffar, Mike Green

Research staff: Kerry Elliott, Tania Neale, Janine Mallinson

Queen's Medical Centre, Derby Road, Nottingham, NG7 2UH, UK

PI: Peter Lanyon
Research staff: Marie-Joséphine Pradere

Addenbrooke's Hospital, Hills Road, Cambridge, CB2 0QQ, UK
PI: Natasha Jordan, Ei Phyu Htut
Research staff: Thelma Mushapaidzi, Donna Abercrombie, Sam Wright, Jane Rowlands

Norfolk and Norwich University Hospital, Colney Lane, Norwich, NR4 7UY, UK
PI: Chetan Mukhtyar
Research staff: James Kennedy

James Paget Hospital, Lowestoft Road, Great Yarmouth, NR31 6LA, UK
PI: Damodar Makkuni
Research staff: Elva Wilhelmsen

The Queen Elizabeth Hospital, Gayton Road, King's Lynn, PE30 4ET, UK
PI: Michael Kouroupis

West Suffolk Hospital, Hardwick Lane, Bury St Edmunds, IP33 2QZ, UK
PI: Shweta Bhagat
Research staff: Lily John

Ashford and St. Peter's Hospitals, London Road, Ashford, TW15 3AA, UK
PI: Rod Hughes
Research staff: Margaret Walsh, Marie Buckley

Torbay Hospital, Newton Road, Torquay, TQ2 7AA, UK
PI: Kirsten Mackay
Research staff: Tracey Camden-Woodley, Joan Redome, Kirsty Pearce

Lister Hospital, Coreys Mill Lane, Stevenage, SG1 4AB, UK
PI: Thirupathy Marianayagam
Research staff: Carina Cruz, Elizabeth Warner

North Tyneside General Hospital, Rake Lane, North Shields, NE29 8NH, UK
PI: Ishmael Atchia
Research staff: Claire Walker, Karen Black, Stacey Duffy

Royal Lancaster Infirmary/Westmorland General Hospital, Ashton Road, Lancaster, LA1 4RP, UK
PI: Marwan Bukhari
Research staff: Lynda Fothergill, Rebecca Jefferey, Jackie Toomey

Royal Glamorgan Hospital, Ynysmaerdy, Pontyclun, CF72 8XR, UK
PI: Ceril Rhys Dillon
Research staff: Carla Potheary, Lauren Green

Warwick Hospital, Lakin Road, Warwick, CV34 5BW, UK

PI: Tracey Toms

Research staff: Linda Maher

West Middlesex Hospital, Twickenham Road, Isleworth, TW7 6AF, UK

PI: Diana Davis

Research staff: Amrinder Sayan, Mini Thankachen

Royal Devon and Exeter Hospital, Barrack Road, Exeter, EX2 5DW, UK

PI: Mahdi Abusalameh

Research staff: Jessica Record

Birmingham Heartlands Hospital, Bordesley Green, Birmingham, B9 5SS, UK

PI: Asad Khan

Research staff: Sam Stafford

Royal Derby Hospital, Uttoxeter Road, Derby, DE22 3NE, UK

PI: Azza Hussein

Research staff: Clare Williams, Alison Fletcher, Laura Johson, Richard Burnett

Aintree University Hospital, Lower Lane, Liverpool, L9 7AL, UK

PI: Robert Moots

Research staff: Helen Frankland

University Hospital Wishaw, Netherton Street, Wishaw, ML2 0DP, UK

PI: James Dale

Research staff: Karen Black, Kirsten Moar, Carol Hollas

Manchester Royal Infirmary, Oxford, Manchester, M13 9WL, UK

PI: Ben Parker

Research staff: Derek Ridings, Sandhya Eapen, Sindhu John

Bristol Royal Infirmary, Upper Maudlin Street, Bristol, BS2 8HW, UK

PI: Jo Robson

Research staff: Lucy Belle Guthrie, Rose Fyfe, Moira Tait

Christchurch Hospital, Fairmile Road, Christchurch, BH23 2JX, UK

PI: Jonathan Marks

Research staff: Emma Gunter, Rochelle Hernandez

Ninewells Hospital & Medical School, James Arrott Drive, Dundee, DD2 1SG, UK

PI: Smita Bhat

Research staff: Paul Johnston

Poole Hospital, Longfleet Road, Poole, BH15 2JB, UK

PI: Muhammad Khurshid
Research staff: Charlotte Barclay

Countess of Chester Hospital, Liverpool Road, Chester, CH2 1UL, UK
PI: Deepti Kapur
Research staff: Helen Jeffrey, Anna Hughes, Lauren Slack

Nevill Hall Hospital, Brecon Road, Abergavenny, NP7 7EG, UK
PI: Eleri Thomas
Research staff: Anna Royon, Angela Hall

Derriford Hospital, Derriford Road, Plymouth, PL6 8DH, UK
PI: Jon King
Research staff: Sindi Nyathi

University College Hospital, Euston Road, London, NW1 2BU, UK
PI: Vanessa Morris, Madhura Castelino
Research staff: Ellie Hawkins, Linda Tomson

Royal Free Hospital, Pond Street, London, NW3 2QY, UK
PI: Animesh Singh
Research staff: Annalyn Nunag, Stella O'Connor

Darlington Memorial Hospital, Hollyhurst Road, Darlington, DL3 6HX, UK
PI: Nathan Rushby
Research staff: Nicola Hewitson

Leicester Royal Infirmary, Infirmary Square, Leicester, LE1 WW, UK
PI: Kenny O'Sunmboye
Research staff: Adam Lewszuk, Louise Boyles

Royal Alexandra Hospital/Vale of Leven Hospital/Inverclyde Royal Hospital, Great Western Road, Glasgow, G12 0XH, UK
PI: Martin Perry

Royal Hampshire County Hospital, Romsey Road, Winchester, SO22 5DG, UK
PI: Emma Williams
Research staff: Christine Graver, Emmanuel Defever

Salford Royal Hospital, Stott Lane, Salford, M6 8HD, UK
PI: Sanjeet Kamanth
Research staff: Dominic Kay, Joe Ogor, Louise Winter

Minerva Health Centre, Lowthorpe Rd, Preston PR1 6SB, UK
PI: Sarah Horton
Research staff: Gillian Welch, Kath Hollinshead

Hammersmith Hospital, Du Cane Road, London, W12 0HS, UK

PI: James Peters

Research nurses: Julius Labao, Andrea Dmello

St Helens Hospital, Marshalls Cross Rd, Saint Helens WA9 3DA, UK

PI: Julie Dawson

Research staff: Denise Graham

Queen Elizabeth the Queen Mother Hospital, Ramsgate Rd, Margate CT9 4AN, UK

PI: Denise De Lord

Research staff: Jo Deery, Tracy Hazelton